

# Estimating the Role of Bag Constant and Modified Theory on Anisotropic Stellar Models

Tayyab Naseer <sup>\*</sup> and M. Sharif <sup>†</sup>

Department of Mathematics and Statistics, The University of Lahore,  
1-KM Defence Road Lahore-54000, Pakistan.

## Abstract

In this article, we are devoted to discuss different compact stars admitting anisotropic interiors in a particular modified theory of gravity. For this purpose, a spherically symmetric metric is adopted to formulate the field equations corresponding to two different  $f(\mathcal{R}, \mathcal{T}, \mathcal{Q})$  models, where  $\mathcal{Q} = \mathcal{R}_{\alpha\gamma}\mathcal{T}^{\alpha\gamma}$ . Since the field equations contain extra degrees of freedom, we choose Finch-Skea metric and MIT bag model equation of state to make them solvable. We also use matching conditions to calculate a constant triplet in the chosen ansatz. The resulting solutions are then graphically analyzed for particular values of the bag constant and model parameter in the interior of 4U 1820-30 compact star. The viability and stability of the modified models are also checked through certain tests. Further, we calculate the values of model parameter through the vanishing radial pressure constraint that correspond to the observed data (radii and masses) of eight different star candidates. Finally, we conclude that our models I and II are in well-agreement with the conditions needed for physically relevant interiors to exist.

**Keywords:**  $f(\mathcal{R}, \mathcal{T}, \mathcal{Q})$  gravity; Compact model; Stability; Anisotropy.  
**PACS:** 04.20.Jb; 03.50.De; 98.80.Jk.

---

<sup>\*</sup>tayyabnaseer48@yahoo.com; tayyab.naseer@math.uol.edu.pk

<sup>†</sup>msharif.math@pu.edu.pk

# 1 Introduction

General Relativity (GR) has long been considered the prevailing gravitational theory within the scientific community, addressing a multitude of challenges. However, it falls short in providing a comprehensive understanding of the rapid cosmic expansion. To grapple with these enigmatic cosmic phenomena, such as the accelerated expansion and the presence of dark matter, scientists have recently explored various extensions to GR. Recent observations have suggested the existence of a repulsive force responsible for this cosmic acceleration, commonly referred to the dark energy, driving galaxies apart from each other. The  $f(\mathcal{R})$  theory stands as the first ever extension to GR, achieved by a modification of the Einstein-Hilbert action, wherein the Ricci scalar  $\mathcal{R}$  is replaced by its generic function [1]. In the quest to understand celestial structures, researchers have employed various techniques within this modified framework to examine the stability and viability [2]-[5]. Beyond its applications to celestial bodies,  $f(\mathcal{R})$  gravity models have played a pivotal role in addressing different cosmological concerns, including the late-time evolution of the universe, the inflationary era, etc. [6]-[9].

In a study conducted by Bertolami and his colleagues [10], a search to unreveal the cosmos' intriguing facets prompted an exploration of a novel concept of the matter-geometry coupling. For this, they incorporated the impact of geometric properties into the matter Lagrangian within the context of  $f(\mathcal{R})$  theory. This pioneering approach piqued the curiosity of various astronomers, who redirected their focus towards understanding the accelerated expansion of the universe. Building on this foundation, recent developments at the action level have led to the emergence of modified theories of gravity, capturing the keen interest of astrophysicists. Harko et al. [11] introduced the first theory based on this concept, known as  $f(\mathcal{R}, \mathcal{T})$  gravity, with  $\mathcal{T}$  representing the trace of the energy-momentum tensor (EMT). The inclusion of  $\mathcal{T}$  gives rise to non-conservation phenomena and has sparked comprehensive investigations into the physical feasibility of self-gravitating structures, resulting in a plethora of noteworthy findings [12]-[21]. Haghani et al. [22] introduced a more intricate functional that depends on  $\mathcal{R}$ ,  $\mathcal{T}$  and  $\mathcal{R}_{\alpha\gamma}\mathcal{T}^{\alpha\gamma}$ . Within this framework, they delved into the study of a cosmic era marked by exponential expansion and explored three different models to assess their physical viability. To further enrich their analysis, they employed the Lagrange multiplier technique to compute conserved EMT within this theory.

The development of this modified proposal hinges on the incorporation of the factor  $\mathcal{Q}$  to enforce a robust non-minimal matter-geometry coupling in self-gravitating systems. Altering the Einstein-Hilbert action offers a potential avenue for elucidating the roles of dark energy and dark matter without relying on exotic fluid distributions. While alternative extensions of GR, such as  $f(\mathcal{R}, \mathcal{L}_m)$  and  $f(\mathcal{R}, \mathcal{T})$  gravitational theories, also include matter Lagrangian with arbitrary interactions, their functionals may not be considered the most generalized forms providing a comprehensive understanding of the impact of the coupling on self-gravitating objects in certain scenarios. Notably, in the case where the internal composition of a star exhibits  $\mathcal{T} = 0$ , the preservation of coupling effects within  $f(\mathcal{R}, \mathcal{T})$  theory fades away. However, such phenomenon does not occur in the context of  $f(\mathcal{R}, \mathcal{T}, \mathcal{Q})$  gravity. The non-conserved energy-momentum tensor in this theory results in an additional force, leading to an end of test particles' motion along geodesic paths. This force also contributes to elucidating galactic rotation curves.

Sharif and Zubair [23] adopted a different approach, investigating two mathematical models  $\mathcal{R} + \beta\mathcal{Q}$  and  $\mathcal{R}(1 + \beta\mathcal{Q})$  with distinct choices for the fluid Lagrangian, specifically  $\mathcal{L}_m = \rho$  and  $-P$ . In doing so, they examined various properties of black holes and their associated thermodynamic laws, subsequently establishing constraints to assess the viability of these models. Odintsov and Saez-Gomez [24] explored the impact of non-constant matter distributions, revealing that such variations can lead to a pure de Sitter universe in the context of  $f(\mathcal{R}, \mathcal{T}, \mathcal{Q})$  theory. Ayuso et al. [25] introduced scalar and vector fields to investigate the modified field equations. Their analysis unveiled the intricate non-linearity stemming from conformal and arbitrary non-minimal matter-geometry couplings. The numerical solutions and stability criteria for different models, along with the use of a perturbation function, have been discussed in detail [26]. Notably, the choice of the matter Lagrangian was found to yield diverse results, particularly depending on the radial/tangential components of pressure [27]. Furthermore, the curvature tensor was orthogonally decomposed in terms of  $f(\mathcal{R}, \mathcal{T}, \mathcal{Q})$  EMT and the Weyl tensor, resulting in some scalar functions for both charged and uncharged fluids, which bear significance in the study of celestial systems [28]-[33]. Extracting the solutions of modified field equations through various techniques led to model several anisotropic systems, which were found to be consistent and physically valid [34]-[37].

Within the vast and enigmatic expanse of the cosmos, stars stand as fundamental constituents of our galaxy. Astrophysicists have long been capti-

vated by the composition of these celestial bodies, focusing on the exploration of their evolution. Among these appealing entities, neutron stars emerged as particularly intriguing, stemming from the gravitational collapse of massive stars. They possess a mass ranging from one to three times that of our solar system and hold a dense core comprised of newly formed neutrons. These neutrons exert a pressure capable of counteracting the attractive force of gravity, preventing further collapse. Although the concept of a neutron star was initially postulated in 1934 [38], observational confirmation took several years, as these structures often elude direct detection, emitting insufficient radiations. In addition to neutron stars, the theoretical realm includes another enigmatic entity, the quark star, situated between the extremes of a black hole and a neutron star. These hypothetical objects are believed to contain strange, down and up quarks within their cores [39]-[43].

The matter determinants characterizing self-gravitating interiors, whether isotropic or anisotropic, are typically described in terms of the energy density and pressure. These attributes are interrelated in some specific way, with one of the well-established constraint being the MIT bag model equation of state (EoS) [44]. Notably, the bag model effectively captures the characteristics of quark star-like structures such as 4U 1820-30, RXJ 185635-3754, PSR 0943+10, Her X-1, SAX J 1808.4-3658, 4U 1728-34, etc. On the other hand, such a description is not attainable with a neutron star EoS [45]. Physicists have extensively employed the MIT bag model to unreveal the inner composition of strange systems [46]-[50]. Demorest et al. [51] conducted a detailed analysis of the compact structure PSR J1614-2230, concluding that only this model supports such incredibly dense objects. Rahaman et al. [52] further investigated specific stellar compositions using this model in conjunction with an interpolating function, while Sharif and his collaborators [53, 54] extended this work across various modified gravity scenarios from which they yield physically stable models.

Numerous methodologies have been presented in scientific literature to address the challenges posed by the Einstein and modified field equations. These approaches encompass the utilization of a specific EoS, well-defined metric potentials, or a vanishing complexity condition, etc. In the realm of radial/time metric components, Finch-Skea ansatz [55] has garnered considerable attention from researchers as a valuable tool for the investigation of anisotropic compact structures. Banerjee et al. [56] presented a family of interior solutions analogous to BTZ exterior by making use of Finch-Skea metric and found physically viable results even in lower dimensions. Hansraj

and Maharaj [57] produced three different classes of analytic solutions to the Einstein-Maxwell field equations and confirmed the fulfillment of stability criteria. The physical analysis indicated that this analogue can be used to model physically realistic charged compact stars. Researchers, both within the realms of GR and in modified theories, have delved into this particular metric solution through different approaches like the gravitational decoupling and the consideration of complexity factor, etc., to discuss self-gravitating charged/uncharged systems [58]-[61].

This study is dedicated to evaluate the physical validity of the Finch-Skea anisotropic solutions within the framework of  $f(\mathcal{R}, \mathcal{T}, \mathcal{R}_{\alpha\gamma}\mathcal{T}^{\alpha\gamma})$  theory. The structure of this paper is as follows. Section **2** provides some basics of this modified theory and explores the corresponding field equations for two distinct models. Additionally, we adopt the MIT bag model EoS to characterize the internal composition of the considered 4U 1820-30 star. In section **3**, we consider the Finch-Skea spacetime and employ junction conditions to calculate the values of an unknown triplet  $(d_1, d_2, d_3)$ , within this ansatz. Section **4** undertakes a graphical examination of the physical characteristics of the resulting solutions by fixing the range of the model parameter. In section **5**, we determine the values of the model parameter which are compatible with the estimated data of different compact stars. Lastly, section **6** provides a summary of our findings.

## 2 Modified $f(\mathcal{R}, \mathcal{T}, \mathcal{R}_{\alpha\gamma}\mathcal{T}^{\alpha\gamma})$ Gravity and MIT Bag Model

The modification of the Einstein-Hilbert action for  $f(\mathcal{R}, \mathcal{T}, \mathcal{R}_{\alpha\gamma}\mathcal{T}^{\alpha\gamma})$  theory (with  $\kappa = 8\pi$ ) is given by [24]

$$\mathcal{S} = \int \sqrt{-g} \left\{ \frac{f(\mathcal{R}, \mathcal{T}, \mathcal{R}_{\alpha\gamma}\mathcal{T}^{\alpha\gamma})}{16\pi} + \mathcal{L}_m \right\} d^4x, \quad (1)$$

where the Ricci scalar is replaced by the modified functional and  $\mathcal{L}_m$  represents the fluid Lagrangian density. Giving variation in the action (1) with respect to the metric tensor yields the field equations in this framework as

$$\mathcal{G}_{\alpha\gamma} = 8\pi \mathcal{T}_{\alpha\gamma}^{(\text{eff})} = \frac{8\pi \mathcal{T}_{\alpha\gamma}}{f_{\mathcal{R}} - \mathcal{L}_m f_{\mathcal{Q}}} + \mathcal{T}_{\alpha\gamma}^{(\text{cor})}, \quad (2)$$

connecting the geometry of the spacetime structure with the fluid content in its interior. The geometry and modified fluid distribution can be expressed by the Einstein tensor  $\mathcal{G}_{\alpha\gamma}$  and EMT  $\mathcal{T}_{\alpha\gamma}^{(\text{eff})}$ , respectively. The functional in the action (1) modifies the fluid sector, containing the EMT of GR along with some correction terms, represented by  $\mathcal{T}_{\alpha\gamma}^{(\text{cor})}$  as

$$\begin{aligned} \mathcal{T}_{\alpha\gamma}^{(\text{cor})} = & -\frac{1}{\left(\mathcal{L}_m f_{\mathcal{Q}} - f_{\mathcal{R}}\right)} \left[ \left( f_{\mathcal{T}} + \frac{1}{2} \mathcal{R} f_{\mathcal{Q}} \right) \mathcal{T}_{\alpha\gamma} - \left\{ \mathcal{L}_m f_{\mathcal{T}} - \frac{\mathcal{R}}{2} \left( \frac{f}{\mathcal{R}} - f_{\mathcal{R}} \right) \right. \right. \\ & + \frac{1}{2} \nabla_{\varrho} \nabla_{\sigma} (f_{\mathcal{Q}} \mathcal{T}^{\varrho\sigma}) \Big\} g_{\alpha\gamma} - \frac{1}{2} \square (f_{\mathcal{Q}} \mathcal{T}_{\alpha\gamma}) - (g_{\alpha\gamma} \square - \nabla_{\alpha} \nabla_{\gamma}) f_{\mathcal{R}} \\ & \left. \left. - 2 f_{\mathcal{Q}} \mathcal{R}_{\varrho(\alpha} \mathcal{T}_{\gamma)}^{\varrho} + \nabla_{\varrho} \nabla_{(\alpha} [\mathcal{T}_{\gamma)}^{\varrho} f_{\mathcal{Q}}] + 2 (f_{\mathcal{Q}} \mathcal{R}^{\varrho\sigma} + f_{\mathcal{T}} g^{\varrho\sigma}) \frac{\partial^2 \mathcal{L}_m}{\partial g^{\alpha\gamma} \partial g^{\varrho\sigma}} \right] \right], \quad (3) \end{aligned}$$

where  $f_{\mathcal{R}}$ ,  $f_{\mathcal{T}}$  and  $f_{\mathcal{Q}}$  are the partial derivatives of the functional  $f(\mathcal{R}, \mathcal{T}, \mathcal{Q})$  with reference to its arguments. Also, we represent the covariant derivative and D'Alambert operator by  $\nabla_{\varrho}$  and  $\square \equiv \frac{1}{\sqrt{-g}} \partial_{\alpha} (\sqrt{-g} g^{\alpha\gamma} \partial_{\gamma})$ , respectively. Moreover, the matter Lagrangian for such fluid distributions can be taken as  $\mathcal{L}_m = -\rho$ , where  $\rho$  is the energy density. This leads to the vanishing of the last term of Eq.(3) [22]. The equivalence principle is broken in this theory due to the non-conservation of the fluid EMT (i.e.,  $\nabla_{\alpha} \mathcal{T}^{\alpha\gamma} \neq 0$ ) until we involve an additional force. This force affects the motion of particles in the self-gravitating systems, changing their path from geodesic to non-geodesic. Consequently, we obtain

$$\begin{aligned} \nabla^{\alpha} \mathcal{T}_{\alpha\gamma} = & \frac{2}{2f_{\mathcal{T}} + \mathcal{R} f_{\mathcal{Q}} + 16\pi} \left[ \nabla_{\alpha} (f_{\mathcal{Q}} \mathcal{R}^{\varrho\alpha} \mathcal{T}_{\varrho\gamma}) - \mathcal{G}_{\alpha\gamma} \nabla^{\alpha} (f_{\mathcal{Q}} \mathcal{L}_m) + \nabla_{\gamma} (\mathcal{L}_m f_{\mathcal{T}}) \right. \\ & \left. - \frac{1}{2} \nabla_{\gamma} \mathcal{T}^{\varrho\sigma} (f_{\mathcal{T}} g_{\varrho\sigma} + f_{\mathcal{Q}} \mathcal{R}_{\varrho\sigma}) - \frac{1}{2} \{ \nabla^{\alpha} (\mathcal{R} f_{\mathcal{Q}}) + 2 \nabla^{\alpha} f_{\mathcal{T}} \} \mathcal{T}_{\alpha\gamma} \right]. \quad (4) \end{aligned}$$

The EMT serves as a fundamental tool in exploring the internal characteristics and composition of self-gravitating systems, making it particularly indispensable in the field of astrophysics. A myriad of celestial bodies, spanning a wide spectrum of massive structures in the universe, is believed to exhibit pressure anisotropy. Consequently, the EMT assumes paramount importance for astrophysicists engaged in deciphering the intricate details of stellar model evolution. Its application extends beyond the confines of conventional isotropic systems, allowing researchers to gain valuable insights

into the gravitational interactions and behaviors of anisotropic matter distributions. The anisotropic EMT is mathematically defined as follows

$$\mathcal{T}_{\alpha\gamma} = (\rho + P_t)U_\alpha U_\gamma + P_t g_{\alpha\gamma} + (P_r - P_t)V_\alpha V_\gamma, \quad (5)$$

where  $P_t$  and  $P_r$  are the tangential and radial pressures, respectively. Furthermore,  $V_\alpha$  symbolizes the four-vector and  $U_\alpha$  being the four-velocity. The field equations for  $f(\mathcal{R}, \mathcal{T}, \mathcal{Q})$  theory derive the trace as

$$\begin{aligned} & 3\nabla^\varrho\nabla_\varrho f_{\mathcal{R}} - \mathcal{T}(8\pi + f_{\mathcal{T}}) - \mathcal{R} \left( \frac{\mathcal{T}}{2}f_{\mathcal{Q}} - f_{\mathcal{R}} \right) + \frac{1}{2}\nabla^\varrho\nabla_\varrho(f_{\mathcal{Q}}\mathcal{T}) \\ & + \nabla_\alpha\nabla_\varrho(f_{\mathcal{Q}}\mathcal{T}^{\alpha\varrho}) - 2f + (\mathcal{R}f_{\mathcal{Q}} + 4f_{\mathcal{T}})\mathcal{L}_m + 2\mathcal{R}_{\alpha\varrho}\mathcal{T}^{\alpha\varrho}f_{\mathcal{Q}} \\ & - 2g^{\gamma\sigma}\frac{\partial^2\mathcal{L}_m}{\partial g^{\gamma\sigma}\partial g^{\alpha\varrho}}(f_{\mathcal{T}}g^{\alpha\varrho} + f_{\mathcal{Q}}R^{\alpha\varrho}) = 0. \end{aligned}$$

The  $f(\mathcal{R}, \mathcal{T})$  gravity is attained from the above equation when setting  $f_{\mathcal{Q}}$  to zero. In addition,  $f_{\mathcal{T}} = 0$  results in the  $f(\mathcal{R})$  theory.

The line element allows us to explore the gravitational field and the way it warps spacetime within massive objects. It plays a pivotal role in describing the conditions prevailing in the interior regions of stars, which are essential for comprehending their structure, evolution, and ultimately, their fate. In this regard, we consider the interior metric representing static spherical spacetime as follows

$$ds^2 = -e^{A_1}dt^2 + e^{A_2}dr^2 + r^2d\theta^2 + r^2\sin^2\theta d\phi^2, \quad (6)$$

where  $A_1 = A_1(r)$  and  $A_2 = A_2(r)$ . The four quantities now take the form

$$V^\alpha = \delta_1^\alpha e^{-\frac{A_2}{2}}, \quad U^\alpha = \delta_0^\alpha e^{-\frac{A_1}{2}}, \quad (7)$$

satisfying  $U^\alpha U_\alpha = -1$  and  $V^\alpha U_\alpha = 0$ .

Our universe is presently undergoing a rapid expansion phase and consists of a vast number of stars existing in a non-linear realm. However, studying their behavior through linear analysis can provide valuable insights for astronomers seeking to comprehend the formation of these massive structures more effectively. Moreover, the non-minimally matter-geometry coupled term  $\mathcal{R}_{\alpha\gamma}\mathcal{T}^{\alpha\gamma}$  makes this theory significantly complicated in comparison with  $f(\mathcal{R}, \mathcal{L}_m)$  and  $f(\mathcal{R}, \mathcal{T})$  scenarios. The motivation behind exploring such coupling in the realm of theoretical physics stems from a desire to refine our understanding of the fundamental interactions shaping the universe. This

coupling involves the intricate interplay between matter fields and the geometry of spacetime, offering a nuanced perspective beyond the conventional minimal coupling scenarios. Researchers are driven by the quest to figure out the mysteries of cosmic evolution through such interactions. Non-minimal coupling models may provide a more comprehensive framework to describe phenomena like dark matter and dark energy, offering potential insights into the accelerated expansion of the universe. To address this, we shall examine two specific functional forms as follows [22]

- **Model I:**  $f(\mathcal{R}, \mathcal{T}, \mathcal{R}_{\alpha\gamma}\mathcal{T}^{\alpha\gamma}) = \mathcal{R} + \beta\mathcal{R}_{\alpha\gamma}\mathcal{T}^{\alpha\gamma}$ ,
- **Model II:**  $f(\mathcal{R}, \mathcal{T}, \mathcal{R}_{\alpha\gamma}\mathcal{T}^{\alpha\gamma}) = \mathcal{R}(1 + \beta\mathcal{R}_{\alpha\gamma}\mathcal{T}^{\alpha\gamma})$ ,

where  $\beta$  denotes a real-valued coupling parameter. It is worth noting that various values of this parameter, well within the observed range, ensure the physical viability of compact star models. Haghani et al. [22] extensively examined these models and explored the evolution of the scale factor as well as deceleration parameter. They deduced that when  $\beta > 0$ , the solution exhibits an oscillatory behavior characterized by alternating phases of expansion and contraction. This dynamic pattern reflects the influence of positive energy density on the evolution of the system. Conversely, when  $\beta < 0$ , the evolution of the universe takes on a different character, with the scale factor demonstrating a dependence of a hyperbolic cosine function. By focusing on these models, Sharif and Zubair [23] delved into isotropic distributions, deriving scientifically acceptable values for the coupling parameter. The value of  $\mathcal{Q}$  in terms of geometric components is given by

$$\begin{aligned} \mathcal{Q} = & e^{-A_2} \left[ \frac{\rho}{4} \left( A_1'^2 - A_1'A_2' + 2A_1'' + \frac{4A_1'}{r} \right) + P_t \left( \frac{A_2'}{r} - \frac{A_1'}{r} + \frac{2e^{A_2}}{r^2} - \frac{2}{r^2} \right) \right. \\ & \left. - \frac{P_r}{4} \left( A_1'^2 - A_1'A_2' + 2A_1'' + \frac{4A_2'}{r} \right) \right], \end{aligned}$$

where prime shows differentiation with respect to  $r$ .

The modified model I yields the independent field equations (2) for the anisotropic fluid (5) given by

$$\begin{aligned} 8\pi\rho = & e^{-A_2} \left[ \frac{A_2'}{r} + \frac{e^{A_2}}{r^2} - \frac{1}{r^2} + \beta \left\{ \rho \left( \frac{3A_1'A_2'}{8} - \frac{A_1'^2}{8} + \frac{A_2'}{r} + \frac{e^{A_2}}{r^2} - \frac{3A_1''}{4} - \frac{3A_1'}{2r} \right. \right. \right. \right. \\ & \left. \left. \left. \left. - \frac{1}{r^2} \right) - \rho' \left( \frac{A_2'}{4} - \frac{1}{r} - A_1' \right) + \frac{\rho''}{2} + P_r \left( \frac{A_1'A_2'}{8} - \frac{A_1'^2}{8} - \frac{A_1''}{4} + \frac{A_2'}{2r} + \frac{A_2''}{2} \right. \right. \right. \right. \\ & \left. \left. \left. \left. - \frac{1}{r^2} \right) \right) \right] \end{aligned}$$

$$-\frac{3A_2'^2}{4}\Big) + \frac{5A_2'P_r'}{4} - \frac{P_r''}{2} + P_t\left(\frac{A_2'}{2r} - \frac{A_1'}{2r} + \frac{3e^{A_2}}{r^2} - \frac{1}{r^2}\right) - \frac{P_t'}{r}\Big\}\Big], \quad (8)$$

$$8\pi P_r = e^{-A_2} \left[ \frac{A_1'}{r} - \frac{e^{A_2}}{r^2} + \frac{1}{r^2} + \beta \left\{ \rho \left( \frac{A_1'A_2'}{8} + \frac{A_1'^2}{8} - \frac{A_1''}{4} - \frac{A_1'}{2r} \right) - \frac{A_1'\rho'}{4} - P_r \right. \right. \\ \times \left( \frac{5A_1'^2}{8} - \frac{7A_1'A_2'}{8} + \frac{5A_1''}{4} - \frac{7A_2'}{2r} + \frac{A_1'}{r} - A_2'^2 - \frac{e^{A_2}}{r^2} + \frac{1}{r^2} \right) + P_r'\left( \frac{A_1'}{4} + \frac{1}{r} \right) \\ \left. \left. - P_t\left( \frac{A_2'}{2r} - \frac{A_1'}{2r} + \frac{3e^{A_2}}{r^2} - \frac{1}{r^2} \right) + \frac{P_t'}{r} \right\} \right], \quad (9)$$

$$8\pi P_t = e^{-A_2} \left[ \frac{A_1'^2}{4} - \frac{A_1'A_2'}{4} + \frac{A_1''}{2} - \frac{A_2'}{2r} + \frac{A_1'}{2r} + \beta \left\{ \rho \left( \frac{A_1'^2}{8} + \frac{A_1'A_2'}{8} - \frac{A_1''}{4} - \frac{A_1'}{2r} \right) \right. \right. \\ - \frac{A_1'\rho'}{4} + P_r\left( \frac{A_1'^2}{8} - \frac{A_1'A_2'}{8} + \frac{A_1''}{4} - \frac{A_2'}{2r} - \frac{A_2''}{2} + \frac{3A_2'^2}{4} \right) - \frac{5A_2'P_r'}{4} + \frac{P_r''}{2} \\ \left. \left. - P_t\left( \frac{A_1'^2}{4} - \frac{A_1'A_2'}{4} + \frac{A_1''}{2} - \frac{A_2'}{r} + \frac{A_1'}{r} \right) - P_t'\left( \frac{A_2'}{4} - \frac{A_1'}{4} - \frac{3}{r} \right) + \frac{P_t''}{2} \right\} \right]. \quad (10)$$

On the other hand, they become for model II as

$$8\pi\rho = e^{-A_2} \left[ \frac{A_2'}{r} + \frac{e^{A_2}}{r^2} - \frac{1}{r^2} + \beta \left\{ \rho \left( \left( \frac{A_2'}{r} + \frac{e^{A_2}}{r^2} - \frac{1}{r^2} \right) \tau_1 - \mathcal{R} \left( \frac{1}{r^2} - \frac{A_2'}{r} - \frac{e^{A_2}}{r^2} \right. \right. \right. \right. \\ + \frac{\mathcal{R}e^{A_2}}{2} - \frac{3A_1'^2}{8} - \frac{3A_1'}{2r} + \frac{5A_1'A_2'}{8} - \frac{3A_1''}{4} \right) + \mathcal{R}' \left( \frac{A_2'}{2} - \frac{1}{r} \right) - \frac{\mathcal{R}''}{2} - \tau_4 \left( \frac{2}{r} \right. \\ \left. - \frac{A_2'}{2} \right) - \tau_7 \Big) + \rho' \left( \tau_1 \left( \frac{A_2'}{2} - \frac{2}{r} \right) - \mathcal{R} \left( \frac{1}{r} - \frac{A_2'}{4} \right) - \mathcal{R}' - 2\tau_4 \right) - \rho'' \left( \tau_1 \right. \\ \left. + \frac{\mathcal{R}}{2} \right) - P_r \left( \left( \frac{1}{r^2} - \frac{A_2'}{r} - \frac{e^{A_2}}{r^2} \right) \tau_2 + \mathcal{R} \left( \frac{A_1'^2}{8} - \frac{1}{r^2} - \frac{A_1'A_2'}{8} + \frac{A_2'}{2r} + \frac{A_1''}{4} \right) \right. \\ \left. - \mathcal{R}' \left( \frac{2}{r} - \frac{A_2'}{2} \right) - \frac{\mathcal{R}''}{2} + \tau_5 \left( \frac{2}{r} - \frac{A_2'}{2} \right) + \tau_8 \right) - P_r' \left( \tau_2 \left( \frac{2}{r} - \frac{A_2'}{2} \right) + \mathcal{R} \right. \\ \times \left( \frac{A_2'}{4} - \frac{2}{r} \right) - \mathcal{R}' + 2\tau_5 \Big) - P_r'' \left( \tau_2 - \frac{\mathcal{R}}{2} \right) - P_t \left( \left( \frac{1}{r^2} - \frac{A_2'}{r} - \frac{e^{A_2}}{r^2} \right) \tau_3 \right. \\ \left. + \mathcal{R} \left( \frac{A_1'}{2r} + \frac{1}{r^2} - \frac{A_2'}{2r} \right) + \frac{\mathcal{R}'}{r} + \tau_6 \left( \frac{2}{r} - \frac{A_2'}{2} \right) + \tau_9 \right) - P_t' \left( \tau_3 \left( \frac{2}{r} - \frac{A_2'}{2} \right) \right. \\ \left. + \frac{\mathcal{R}}{2} + 2\tau_6 \right) - P_t'' \tau_3 \Big\} \right], \quad (11)$$

$$\begin{aligned}
8\pi P_r = & e^{-A_2} \left[ \frac{A'_1}{r} - \frac{e^{A_2}}{r^2} + \frac{1}{r^2} + \beta \left\{ \rho \left( \left( \frac{A'_1}{r} - \frac{e^{A_2}}{r^2} + \frac{1}{r^2} \right) \tau_1 - \mathcal{R} \left( \frac{e^{A_2}}{r^2} - \frac{1}{r^2} - \frac{A'_1}{r} \right. \right. \right. \right. \right. \right. \\
& + \frac{A''_1}{8} + \frac{A'_1}{2r} - \frac{A'_1 A_2'}{8} + \frac{A''_1}{4} \left. \right) + \frac{\mathcal{R}' A'_1}{4} + \tau_4 \left( \frac{2}{r} + \frac{A'_1}{2} \right) \left. \right) + \rho' \left( \tau_1 \left( \frac{2}{r} + \frac{A'_1}{2} \right) \right. \\
& + \frac{\mathcal{R} A'_1}{4} \left. \right) + P_r \left( \left( \frac{1}{r^2} + \frac{A'_1}{r} - \frac{e^{A_2}}{r^2} \right) \tau_2 - \mathcal{R} \left( \frac{\mathcal{R} e^{A_2}}{2} - \frac{3A''_1}{8} + \frac{1}{r^2} + \frac{A'_1}{r} + \frac{3A_2'}{2r} \right. \right. \\
& + \frac{3A'_1 A_2'}{8} - \frac{3A''_1}{4} \left. \right) - \mathcal{R}' \left( \frac{1}{r} + \frac{A'_1}{4} \right) + \tau_5 \left( \frac{2}{r} + \frac{A'_1}{2} \right) \left. \right) + P'_r \left( \tau_2 \left( \frac{2}{r} + \frac{A'_1}{2} \right) \right. \\
& - \mathcal{R} \left( \frac{A'_1}{4} + \frac{1}{r} \right) \left. \right) - P_t \left( \left( \frac{A'_1}{r} + \frac{e^{A_2}}{r^2} - \frac{1}{r^2} \right) \tau_3 + \mathcal{R} \left( \frac{A_2'}{2r} - \frac{1}{r^2} - \frac{A'_1}{2r} \right) + \frac{\mathcal{R}'}{r} \right. \\
& - \tau_6 \left( \frac{2}{r} + \frac{A'_1}{2} \right) \left. \right) + P'_t \left( \tau_3 \left( \frac{2}{r} + \frac{A'_1}{2} \right) - \frac{\mathcal{R}}{2} \right) \left. \right\} \right], \tag{12}
\end{aligned}$$

$$\begin{aligned}
8\pi P_t = & e^{-A_2} \left[ \frac{A_1''}{2} - \frac{A_1'A_2'}{4} + \frac{A_1'^2}{4} + \frac{A_1'}{2r} - \frac{A_2}{2r} + \beta \left\{ \rho \left( \tau_1 \left( \frac{A_1''}{2} - \frac{A_1'A_2'}{4} + \frac{A_1'^2}{4} \right. \right. \right. \right. \right. \\
& + \frac{A_1'}{2r} - \frac{A_2}{2r} \left. \right) - \mathcal{R} \left( \frac{A_1'A_2'}{8} - \frac{A_1''}{4} - \frac{A_1'^2}{8} + \frac{A_2'}{2r} \right) - \left( \frac{A_2'}{2} - \frac{1}{r} - \frac{A_1'}{2} \right) \tau_4 + \tau_7 \\
& - \frac{\mathcal{R}'A_1'}{4} \left. \right) - \rho' \left( \tau_1 \left( \frac{A_2'}{2} - \frac{1}{r} - \frac{A_1'}{2} \right) + \frac{\mathcal{R}A_1'}{4} - 2\tau_4 \right) + \rho''\tau_1 - P_r \left( \left( \frac{A_2'}{2r} \right. \right. \\
& - \frac{A_1''}{2} - \frac{A_1'^2}{4} - \frac{A_1'}{2r} + \frac{A_1'A_2'}{4} \left. \right) \tau_2 + \mathcal{R} \left( \frac{A_1'^2}{8} + \frac{A_1'}{2r} - \frac{A_1'A_2'}{8} + \frac{A_1''}{4} \right) + \mathcal{R}' \\
& \times \left( \frac{A_1'}{2} + \frac{1}{r} - \frac{A_2'}{4} \right) + \frac{\mathcal{R}''}{2} + \tau_5 \left( \frac{A_2'}{2} - \frac{1}{r} - \frac{A_1'}{2} \right) - \tau_8 \left. \right) - P_r' \left( \tau_2 \left( \frac{A_2'}{2} \right. \right. \\
& - \frac{1}{r} - \frac{A_1'}{2} \left. \right) + \mathcal{R} \left( \frac{A_1'}{2} + \frac{1}{r} - \frac{A_2'}{4} \right) + \mathcal{R}' - 2\tau_5 \left. \right) + P_r'' \left( \tau_2 - \frac{\mathcal{R}}{2} \right) + P_t \left( \tau_3 \right. \\
& \times \left( \frac{A_1''}{2} - \frac{A_1'A_2'}{4} + \frac{A_1'^2}{4} + \frac{A_1'}{2r} - \frac{A_2}{2r} \right) - \mathcal{R} \left( \frac{\mathcal{R}e^{A_2}}{2} - \frac{2}{r^2} + \frac{A_2'}{r} - \frac{A_1'}{r} + \frac{2e^{A_2}}{r^2} \right) \\
& - \mathcal{R}' \left( \frac{A_1'}{4} - \frac{A_2'}{4} \right) - \frac{\mathcal{R}''}{2} - \tau_6 \left( \frac{A_2'}{2} - \frac{1}{r} - \frac{A_1'}{2} \right) + \tau_9 \left. \right) - P_t' \left( \tau_3 \left( \frac{A_2'}{2} - \frac{1}{r} \right. \right. \\
& - \frac{A_1'}{2} \left. \right) + \mathcal{R} \left( \frac{A_1'}{4} - \frac{A_2'}{4} + \frac{2}{r} \right) + \mathcal{R}' - 2\tau_6 \left. \right) + P_t'' \left( \tau_3 - \frac{\mathcal{R}}{2} \right) \left. \right\} \right], \quad (13)
\end{aligned}$$

where  $\tau_i^{s*}$ ,  $i = 1, 2, 3, \dots, 9$  are provided in Appendix A. Misner and Sharp [62] proposed a formula that helps to calculate the mass of self-gravitating

spherical objects. This is given by

$$m(r) = \frac{r}{2} (1 - g^{\alpha\gamma} r_{,\alpha} r_{,\gamma}),$$

giving rise to

$$m(r) = \frac{r}{2} (1 - e^{-A_2}). \quad (14)$$

Within any geometric configuration, physical parameters such as pressure and energy density can be intricately linked through some specific relationships known as EoSs. The end of a massive star's life cycle may result in the formation of a white dwarf, neutron star, or black hole, with neutron stars standing out as particularly captivating celestial formations within our universe. Moreover, under varying density conditions in their cores, these structures can undergo transformations into quark stars or black holes [46, 63, 64]. Notably, these celestial objects boast incredibly dense cores, generating strong gravitational fields around them, despite their relatively small sizes. Since the sets of equations (8)-(10) and (11)-(13) possess matter variables and its derivatives coupled with geometric terms, obtaining solutions for these equations can be a non-trivial task. Consequently, the imposition of certain constraints becomes imperative to derive the requisite solutions. Here, we adopt the MIT bag model EoS to delve into the physical characteristics of diverse quark candidates [44]. We define the quark pressure as

$$P_r = \sum_{\iota=s,u,d} P^\iota - B_c, \quad (15)$$

with  $B_c$  being the bag constant. Further, the subscripts  $s$ ,  $u$  and  $d$  correspond to strange, up and down flavors of quarks, respectively. The quark energy density is linked with its pressure by the amount  $\rho^\iota = 3P^\iota$ . Hence, the total energy density can mathematically be expressed as

$$\rho = \sum_{\iota=s,u,d} \rho^\iota + B_c. \quad (16)$$

Joining the above two equations results in the following

$$P_r = \frac{1}{3} (\rho - 4B_c). \quad (17)$$

Researchers investigated several quark interiors with the help of the above equation and deduced the values of the bag constant which are compatible

with the observed data [65, 66]. Equations (8) and (9) now become after combining with EoS (17) as

$$\rho = \left[ \beta \left( \frac{9A_1''}{8} - \frac{e^{A_2}}{r^2} + \frac{1}{r^2} - \frac{A_2''}{8} - \frac{5A_1'A_2'}{8} - \frac{A_2'^2}{16} - \frac{7A_2'}{2r} + \frac{3A_1'^2}{16} + \frac{7A_1'}{4r} \right) \right. \\ \left. + 8\pi e^{A_2} \right]^{-1} \left[ \frac{3}{4} \left( \frac{A_2'}{r} + \frac{A_1'}{r} \right) + B_c \left\{ 8\pi e^{A_2} - \beta \left( \frac{4A_2'}{r} - \frac{3A_1'^2}{4} - \frac{3A_1''}{2} + \frac{A_2''}{2} \right. \right. \right. \\ \left. \left. \left. + \frac{A_2'^2}{4} + A_1'A_2' - \frac{A_1'}{r} + \frac{e^{A_2}}{r^2} - \frac{1}{r^2} \right) \right\} \right], \quad (18)$$

$$P_r = \left[ \beta \left( \frac{9A_1''}{8} - \frac{e^{A_2}}{r^2} + \frac{1}{r^2} - \frac{A_2''}{8} - \frac{5A_1'A_2'}{8} - \frac{A_2'^2}{16} - \frac{7A_2'}{2r} + \frac{3A_1'^2}{16} + \frac{7A_1'}{4r} \right) \right. \\ \left. + 8\pi e^{A_2} \right]^{-1} \left[ \frac{1}{4} \left( \frac{A_2'}{r} + \frac{A_1'}{r} \right) - B_c \left\{ 8\pi e^{A_2} - \beta \left( \frac{A_1'A_2'}{2} + \frac{A_2'}{r} - \frac{2A_1'}{r} \right. \right. \right. \\ \left. \left. \left. + \frac{e^{A_2}}{r^2} - A_1'' - \frac{1}{r^2} \right) \right\} \right], \quad (19)$$

whilst Eqs.(11) and (12) take the form

$$\rho = \left[ \beta \left\{ \frac{3}{4} \left( \frac{A_2'}{r} + \frac{A_1'}{r} \right) \left( \tau_1 + \frac{\tau_2}{3} \right) + \frac{3}{8} (A_2' + A_1') \left( \tau_4 + \frac{\tau_5}{3} \right) + \mathcal{R} \left( \frac{A_1''}{2} + \frac{A_2'}{4r} \right. \right. \right. \\ \left. \left. \left. - \frac{7A_1'A_2'}{16} + \frac{A_1'^2}{16} + \frac{5A_1'}{4r} - \frac{\mathcal{R}e^{A_2}}{2} \right) + \mathcal{R}' \left( \frac{A_1'}{8} - \frac{1}{2r} + \frac{A_2'}{8} \right) - \frac{\mathcal{R}''}{4} - \frac{\tau_8}{4} \right\} \right. \\ \left. - 8\pi e^{A_2} \right]^{-1} \left[ - \frac{3}{4} \left( \frac{A_2'}{r} + \frac{A_1'}{r} \right) - 8\pi B_c e^{A_2} - \beta B_c \left\{ \left( \frac{A_2'}{r} + \frac{A_1'}{r} \right) \tau_2 - \mathcal{R} \left( \frac{A_1'^2}{2} \right. \right. \right. \\ \left. \left. \left. + \frac{\mathcal{R}e^{A_2}}{2} + \frac{A_1'}{r} + \frac{A_1'A_2'}{4} + \frac{2A_2'}{r} - \frac{A_1''}{2} \right) - \mathcal{R}' \left( \frac{A_1'}{4} - \frac{1}{r} + \frac{A_2'}{4} \right) + \frac{\mathcal{R}''}{2} - \tau_8 \right. \right. \\ \left. \left. + \tau_5 \left( \frac{A_2'}{2} + \frac{A_1'}{2} \right) \right\} \right], \quad (20)$$

$$P_r = \left[ \beta \left\{ \frac{3}{4} \left( \frac{A_2'}{r} + \frac{A_1'}{r} \right) \left( \tau_1 + \frac{\tau_2}{3} \right) + \frac{3}{8} (A_2' + A_1') \left( \tau_4 + \frac{\tau_5}{3} \right) + \mathcal{R} \left( \frac{A_1''}{2} + \frac{A_2'}{4r} \right. \right. \right. \\ \left. \left. \left. - \frac{7A_1'A_2'}{16} + \frac{A_1'^2}{16} + \frac{5A_1'}{4r} - \frac{\mathcal{R}e^{A_2}}{2} \right) + \mathcal{R}' \left( \frac{A_1'}{8} - \frac{1}{2r} + \frac{A_2'}{8} \right) - \frac{\mathcal{R}''}{4} - \frac{\tau_8}{4} \right\} \right. \\ \left. - 8\pi e^{A_2} \right]^{-1} \left[ - \frac{1}{4} \left( \frac{A_2'}{r} + \frac{A_1'}{r} \right) + 8\pi B_c e^{A_2} - \beta B_c \left\{ \left( \frac{A_2'}{r} + \frac{A_1'}{r} \right) \tau_1 + \mathcal{R} \left( \frac{A_1'^2}{4} \right. \right. \right. \\ \left. \left. \left. + \frac{\mathcal{R}e^{A_2}}{4} + \frac{A_1'}{r} + \frac{A_1'A_2'}{4} + \frac{2A_2'}{r} - \frac{A_1''}{2} \right) - \mathcal{R}' \left( \frac{A_1'}{4} - \frac{1}{r} + \frac{A_2'}{4} \right) + \frac{\mathcal{R}''}{2} - \tau_8 \right. \right. \\ \left. \left. + \tau_5 \left( \frac{A_2'}{2} + \frac{A_1'}{2} \right) \right\} \right], \quad (21)$$

$$\begin{aligned}
& -\frac{\mathcal{R}e^{A_2}}{2} + \frac{A_2'}{r} - \frac{A_1'A_2'}{2} + \frac{A_1''}{2} + \frac{2A_1'}{r} \Big) + \mathcal{R}' \left( \frac{A_1'}{4} - \frac{1}{r} + \frac{A_2'}{4} \right) - \frac{\mathcal{R}''}{2} - \tau_7 \\
& + \tau_4 \left( \frac{A_2'}{2} + \frac{A_1'}{2} \right) \Big\} \Big].
\end{aligned} \tag{21}$$

One can determine the tangential pressure for model I by incorporating the energy density (18) and the radial pressure (19) into Eq.(10). Similarly, for model II, this can be obtained by utilizing together Eqs.(13), (20) and (21). In this study, we present solutions to the field equations for both models using MIT bag model, with a particular range of the coupling parameter. This analysis provides valuable insights into the behavior of strange quark celestial bodies.

### 3 Finch-Skea Spacetime and Matching Conditions

Since the field equations still involve extra unknowns, we turn our attention to the Finch-Skea spacetime, an ansatz that has garnered considerable attention in the realm of astrophysics. The metric coefficients of this line element are given by [55]

$$e^{A_1} = \frac{1}{4} (2d_1 + d_2 \sqrt{d_3} r^2)^2, \quad e^{A_2} = d_3 r^2 + 1, \tag{22}$$

comprising a triplet  $(d_1, d_2, d_3)$ , need to be determined. We shall use the matching criteria in the following to determine their values in terms of radius and mass of a compact star. Since multiple metrics have been proposed in the literature, one must check whether the ansatz under consideration is physically acceptable or not. For this, a criteria has been proposed [67] and we take derivatives of both time/radial components in order to verify it as follows

$$\begin{aligned}
A_1'(r) &= \frac{4d_2\sqrt{d_3}r}{d_2\sqrt{d_3}r^2 + 2d_1}, \quad A_1''(r) = \frac{8d_1d_2\sqrt{d_3} - 4d_2^2d_3r^2}{(d_2\sqrt{d_3}r^2 + 2d_1)^2}, \\
A_2'(r) &= \frac{2d_3r}{d_3r^2 + 1}, \quad A_2''(r) = \frac{2d_3}{d_3r^2 + 1} - \frac{4d_3^2r^2}{(d_3r^2 + 1)^2}.
\end{aligned}$$

We observe from the above expressions that  $A'_1(0) = 0 = A'_2(0)$  and  $A''_1(0), A''_2(0) > 0$  everywhere ( $r = 0$  being star's center). Hence, the acceptance of both potentials defined in Eq.(22) is validated.

The matching of the interior and exterior regions at the hypersurface offers a set of conditions that prove to be an immensely valuable tool for understanding the overall structure of celestial bodies. Ensuring a correspondence between the characteristics of both these spacetimes is indeed necessary. This entails considerations such as the charge/uncharge distribution, whether the regions are static or in a state of dynamical evolution, and other relevant parameters. In the light of these factors, the Schwarzschild metric with  $M$  representing the total mass emerges as the most suitable choice for describing the exterior geometry. We take it as

$$ds^2 = - \left( 1 - \frac{2M}{r} \right) dt^2 + \frac{dr^2}{\left( 1 - \frac{2M}{r} \right)} + r^2 d\theta^2 + r^2 \sin^2 \theta d\phi^2. \quad (23)$$

The matching conditions are mainly based on two fundamental forms. The first of them assures the continuity of metric coefficients and their derivatives of both regions across the spherical boundary. This gives

$$g_{tt} \stackrel{\Sigma}{=} e^{A_1(R)} = \frac{1}{4} (2d_1 + d_2 \sqrt{d_3} R^2)^2 = 1 - \frac{2M}{R}, \quad (24)$$

$$g_{rr} \stackrel{\Sigma}{=} e^{A_2(R)} = d_3 R^2 + 1 = \left( 1 - \frac{2M}{R} \right)^{-1}, \quad (25)$$

$$\frac{\partial g_{tt}}{\partial r} \stackrel{\Sigma}{=} A'_1(R) = \frac{4d_2 \sqrt{d_3} R}{2d_1 + d_2 \sqrt{d_3} R^2} = \frac{2M}{R(R - 2M)}. \quad (26)$$

Solving the above equations simultaneously, the triplet is calculated as

$$d_1 = \frac{2R - 5M}{2R\sqrt{R - 2M}}, \quad d_2 = \frac{1}{R^{\frac{3}{2}}} \sqrt{\frac{M}{2}}, \quad d_3 = \frac{2M}{R^2(R - 2M)}. \quad (27)$$

An alternative method for determining these constants is to take the initial two constraints described in Eqs.(24) and (25), in addition to the condition of vanishing radial pressure at the spherical boundary, i.e.,  $P_r \stackrel{\Sigma}{=} 0$ . By employing these three equations, distinct set of values for the triplet can be derived. However, we shall use the later condition for estimating the values of the model parameter.

## 4 Graphical Interpretation of Constructed Solutions

This section is devoted to graphically analyze our both resulting solutions for a particular 4U 1820-30 compact body in this modified theory. The preliminary data of this star is provided as the radius  $R = 9.1 \pm 0.4 \text{ km}$  and mass  $M = 1.58 \pm 0.06 \text{ M}_\odot$  [68]. Further, we conduct a comprehensive analysis of the considered model, encompassing an array of critical properties to ascertain the physical viability of the developed solutions. These properties include the metric potentials, anisotropy, energy bounds, mass and redshift, etc. The investigation also extends to the stability of the obtained models, taking into account the specific range of the model parameter  $\beta$  that can be positive or negative.

There are some of our works in which the positive values of  $\beta$  do not provide physically acceptable results as the behavior of the fluid triplet appears to be the negative [69, 70]. Thus we required to adopt its negative values to obtain physically relevant compact interiors. However, this is not the case in this article. Both positive as well as negative values of this parameter can be chosen that shall later be shown through graphical analysis. Moreover, we plot these physical properties for different values of the bag constant and find good results for  $B_c = 92 \text{ MeV}/fm^3$ . Hence, all the plots in this paper correspond to this value. It is important to emphasize that a valid solution should exhibit metric functions that are not only monotonically increasing but also devoid of singularities. This consistency is clearly evident in the graphical representations of the temporal and radial metric coefficients (22), as illustrated in Figure 1.

### 4.1 Matter Determinants

The concentration of matter within the core of a geometric structure is a fundamental need in order to validate the corresponding solution. This implies that the density and pressures must be maximum and finitely positive in the center and decrease outwards. In this case of anisotropic fluid, the energy density and the radial/tangential pressures are important factors to assess. To this end, we perform a comparative analysis for models I and II in Figure 2. Notably, the analysis reveals that the matter variables exhibit behavior consistent with physically acceptable models. This observation lends

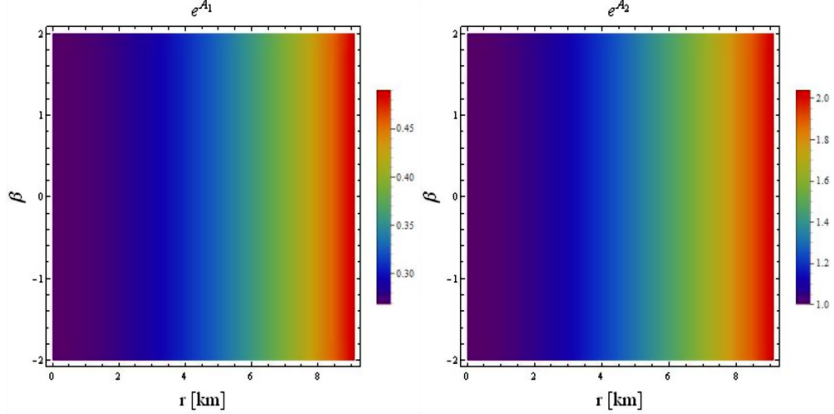


Figure 1: Metric potentials (22) versus  $\beta$  and  $r$ .

support to the presence of highly dense cores within the framework of modified gravity. Examining the first row of Figure 2, it becomes apparent that model I generates slightly dense structures. Moreover, the remaining graphs in the same Figure demonstrate that model II acquires higher values of both pressure components within the considered stellar object. Importantly, the regular conditions for both models are verified and the corresponding plots are included in Figures 3 and 4.

## 4.2 Anisotropic Pressure

The anisotropy is defined by  $\Pi = P_t - P_r$ . This subsection explores the influence of this factor on the structural evolution of the compact star under investigation through a graphical analysis of this phenomenon. The characteristics of anisotropy can be elucidated as follows.

- Anisotropy manifests as an outward expansion when the radial pressure is lower than the tangential pressure.
- Conversely, it manifests as an inward contraction when the tangential pressure falls below the radial pressure.

The anisotropy corresponding to both models I and II is presented in Appendix B. We observe this to be zero at the center from Figure 5 and increasing outwards, exhibiting maximum value at the boundary. It is also found

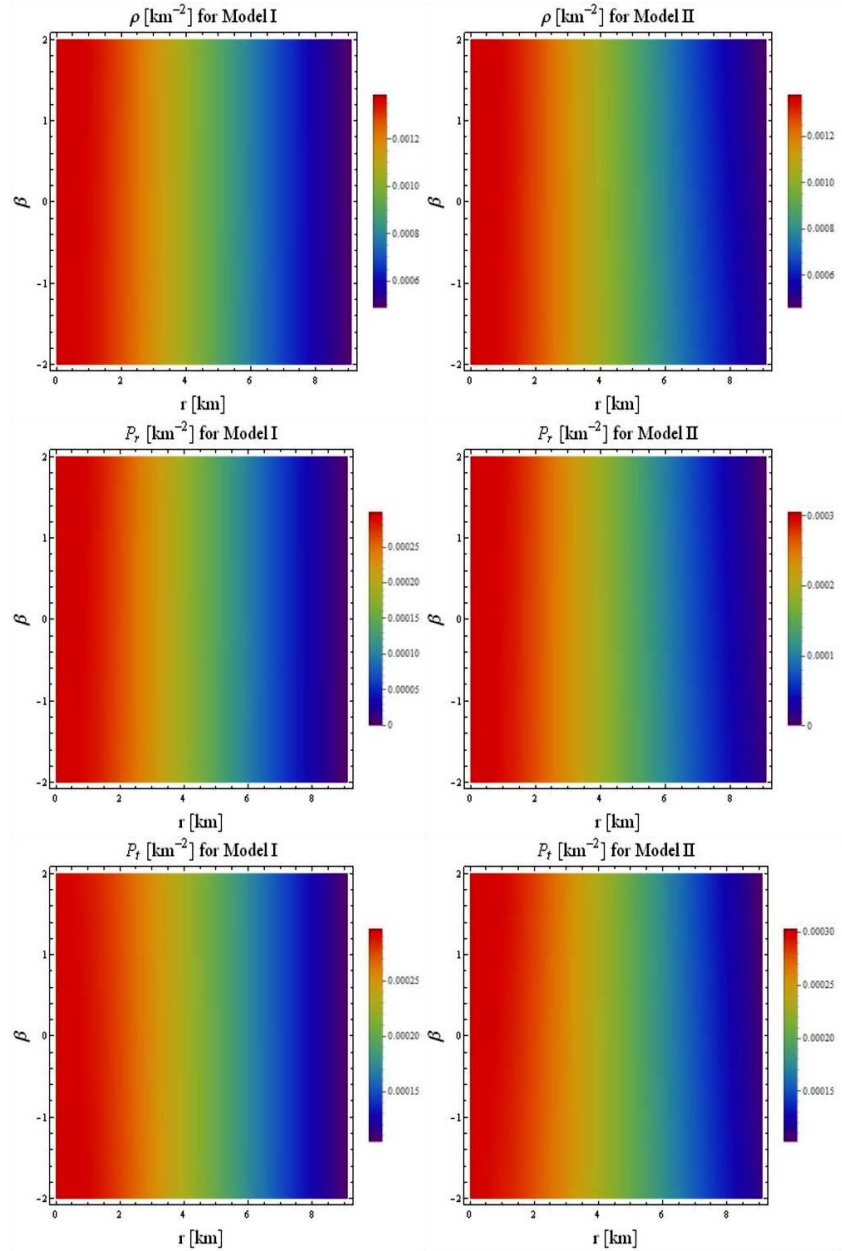


Figure 2: Matter variables versus  $\beta$  and  $r$ .

that the compact structure analogous to the model I possesses a little more anisotropy in comparison with the other model.

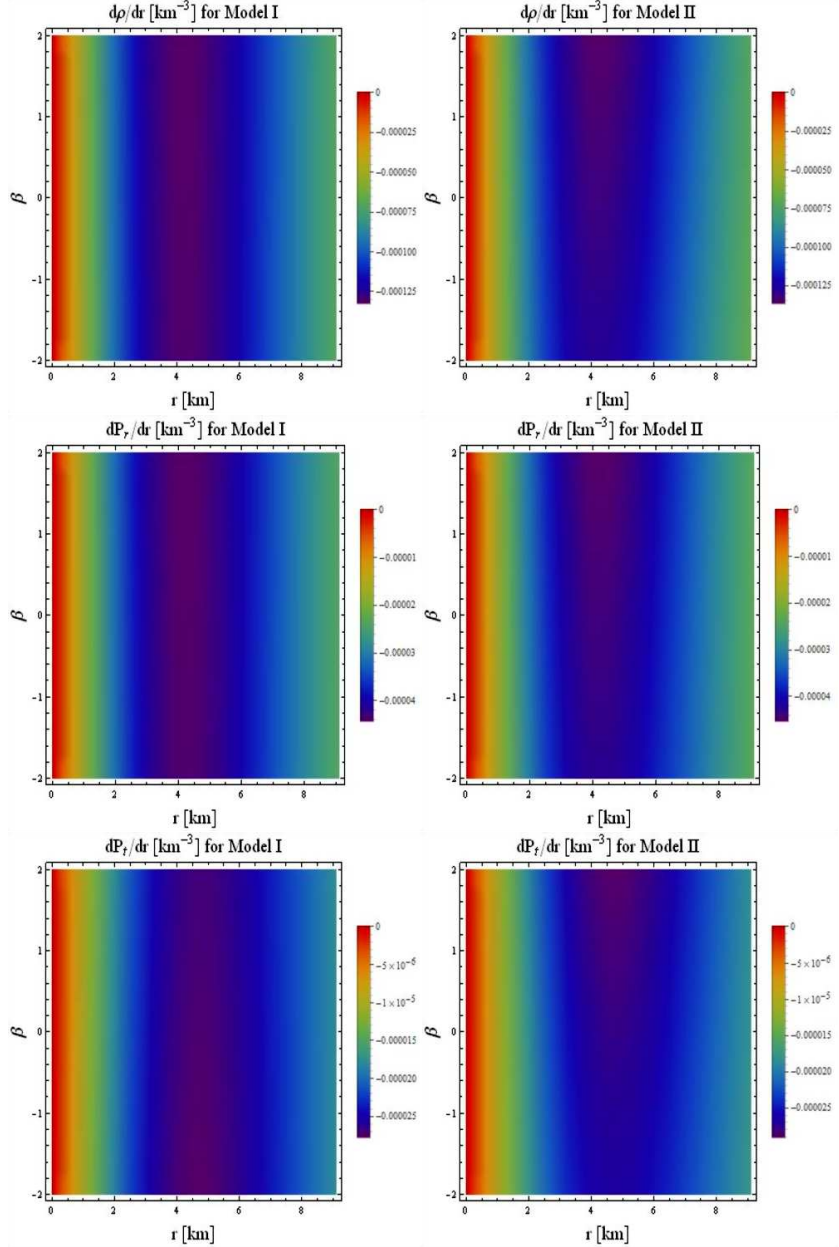


Figure 3: First derivative of matter variables versus  $\beta$  and  $r$ .

### 4.3 Mass, Compactness and Redshift Parameters

We firstly present the mass function of a spherical structure in terms of the geometric quantity (14) that remains same in GR and modified theories.

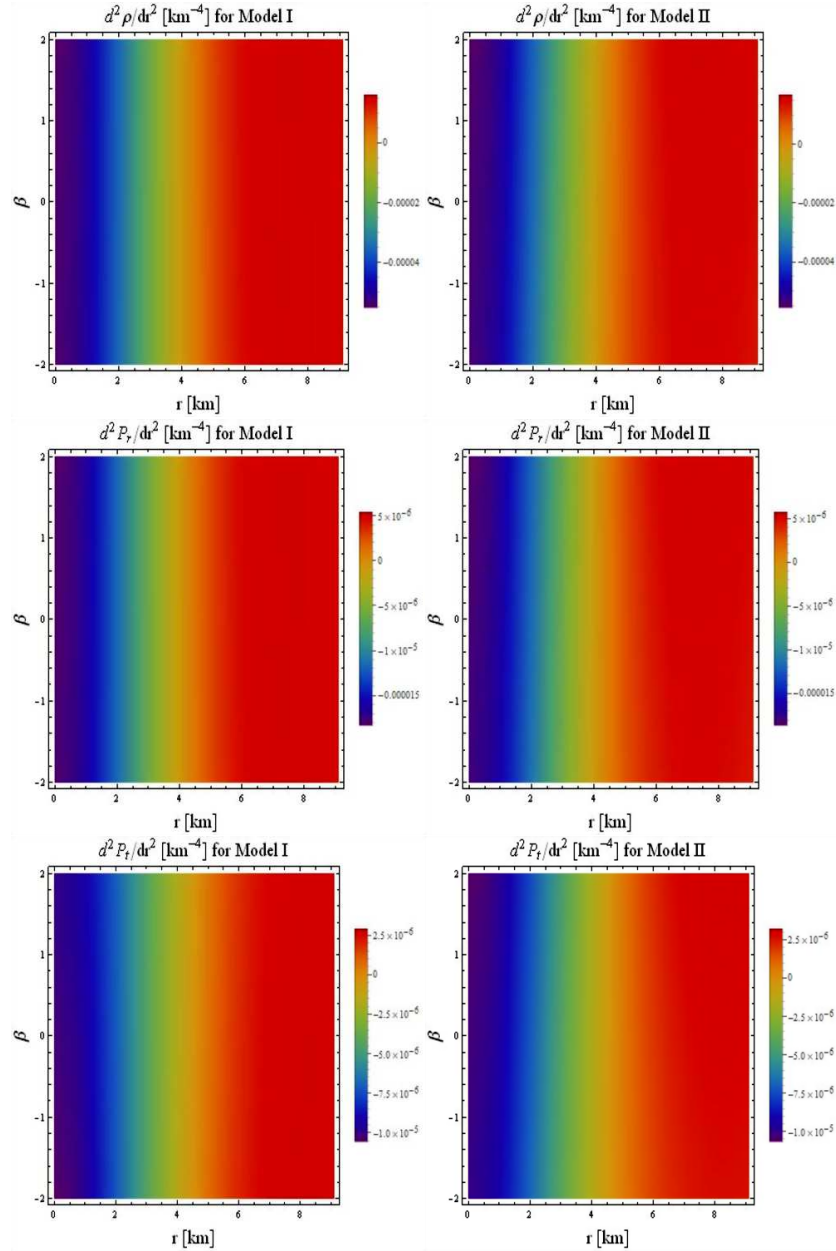


Figure 4: Second derivative of matter variables versus  $\beta$  and  $r$ .

However, the following equation expresses the spherical mass in terms of the energy density possessing modified correction terms, thus, the impact of

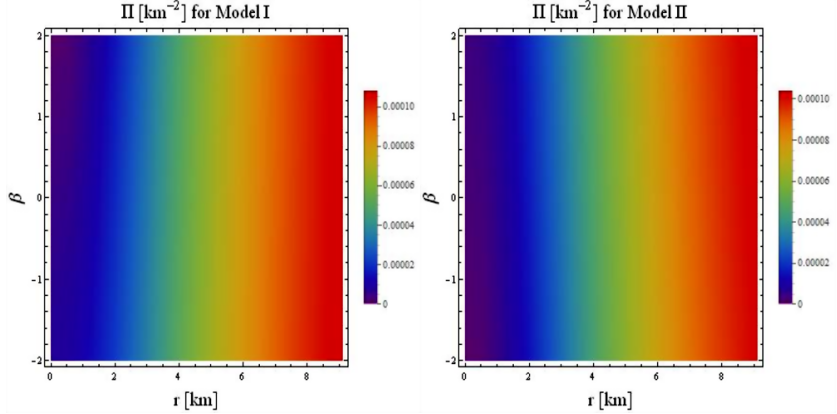


Figure 5: Anisotropy versus  $\beta$  and  $r$ .

modified gravity can be checked. This relation is defined by

$$m(r) = \frac{1}{2} \int_0^R r^2 \rho dr, \quad (28)$$

where  $\rho$  being the effective energy density (possessing the correction terms). We already presented it in Eqs.(18) and (20) analogous to both considered models. Figure 6 (first row) implies that the mass function disappears at  $r = 0$  and increases towards the spherical boundary for both models. Notably, our model I generates a slightly massive structure as compared to that produced by model II.

Numerous physical parameters, including compactness and surface redshift, have been extensively examined in scientific literature to gain insight into the evolution and properties of compact stellar objects. Compactness, for instance, is defined as the ratio of a star's mass to its radius. Buchdahl [71], in his seminal work, proposed a maximum value for compactness (represented by  $\mu$ ) within the framework of a celestial system, setting it at  $\frac{4}{9}$  through meticulous analysis that satisfies matching criteria at the hypersurface ( $r = R$ ).

A massive celestial body, ensconced within a strong gravitational field, emits electromagnetic radiations due to various nuclear reactions occurring within its core. As these radiations traverse space, their wavelengths can stretch, causing a phenomenon known as redshift. The mathematical formu-

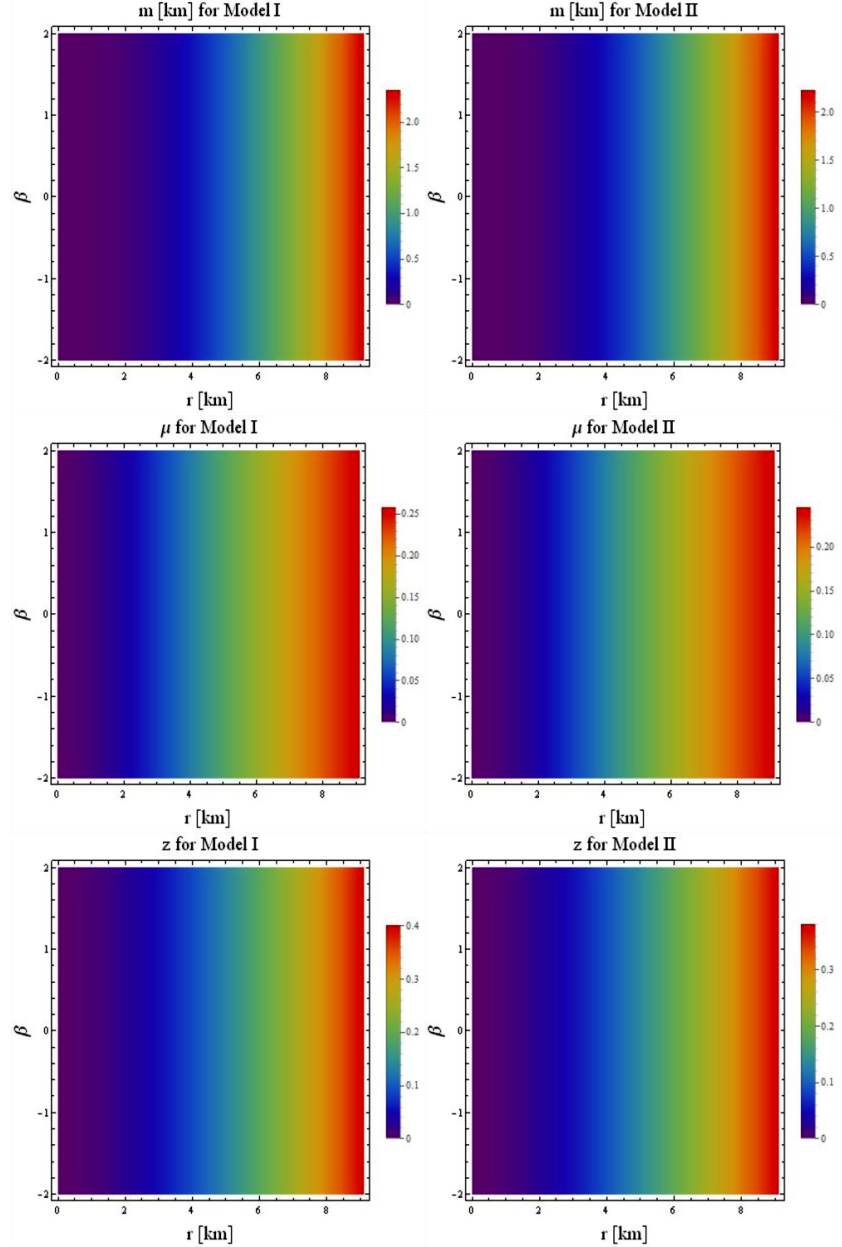


Figure 6: Physical factors versus  $\beta$  and  $r$ .

lation of this parameter is

$$z(r) = \frac{1}{\sqrt{1 - 2\mu(r)}} - 1. \quad (29)$$

while, theoretical models with uniformly distributed matter within such bodies have an upper limit of 2. A noteworthy development emerged in the work of Ivanov [72] who extended this limit to 5.211 for the anisotropic distribution. The second and last rows of Figure 6 confirm both above factors within their suggested bounds.

#### 4.4 Equation of State Parameters

Another essential aspect in assessing the relevancy of the self-gravitating models is to explore the EoS parameters. These equations establish the connection between the density and pressure of the considered fluid distribution. Given that we are working within the anisotropic framework, these equations take the form as

$$\omega_r = \frac{P_r}{\rho}, \quad \omega_t = \frac{P_t}{\rho}. \quad (30)$$

It is crucial that these parameters must fall within the range of  $[0, 1]$  for the viability of stellar matter configurations. The information depicted in Figure 7 offers empirical confirmation that both models I and II adhere to the prescribed range for these parameters.

#### 4.5 Energy Conditions

The inner composition of celestial structures can encompass either normal or exotic fluids. The existence of a normal fluid within a compact star is determined by the energy conditions that rely on various physical parameters, including pressure and energy density. It is essential to consider these conditions when analyzing astronomical systems in modified theories, as the correction terms can have a significant impact on them. Consequently, meeting with the following criteria ensures the formation of a realistic and scientifically sound configuration

- Weak:  $\rho + P_t \geq 0, \quad \rho \geq 0, \quad \rho + P_r \geq 0,$
- Strong:  $\rho + P_r + 2P_t \geq 0,$
- Null:  $\rho + P_t \geq 0, \quad \rho + P_r \geq 0,$
- Dominant:  $\rho \pm P_t \geq 0, \quad \rho \pm P_r \geq 0.$

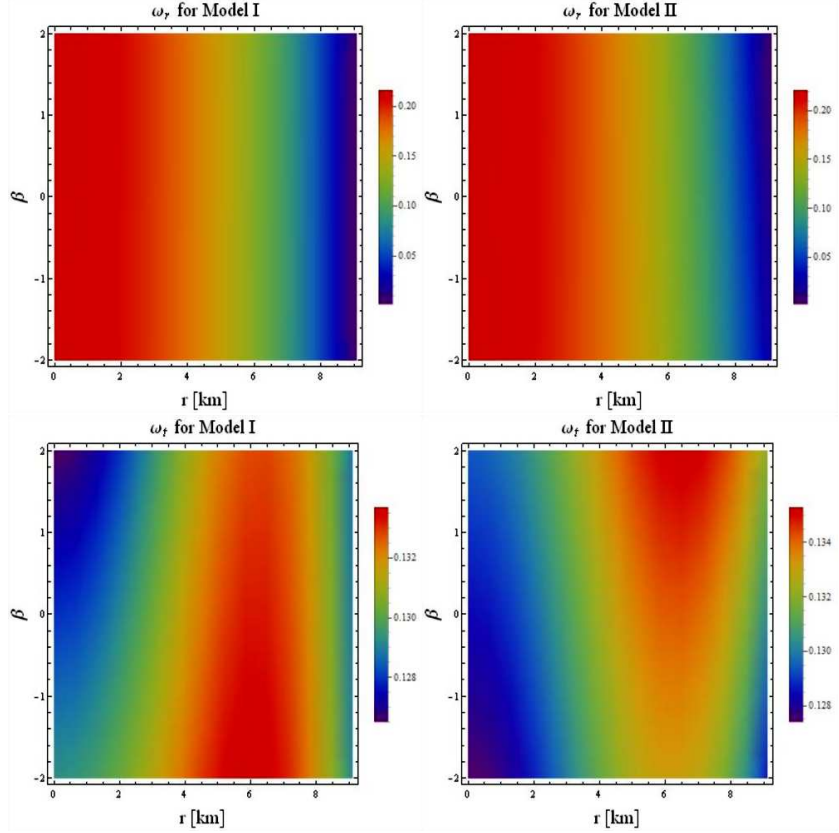


Figure 7: Equation of state parameters versus  $\beta$  and  $r$ .

The graphical representation of these constraints can be observed in Figures 8 and 9, which correspond to models I and II, respectively. All the plots illustrate consistently positive behaviors. Consequently, this suggests that the solutions developed for both  $f(\mathcal{R}, \mathcal{T}, \mathcal{Q})$  models conform to physical viability standards, indicating the presence of normal matter within their respective interiors.

#### 4.6 Tolman-Oppenheimer-Volkoff Equation

The analysis of different fundamental forces is indeed necessary in order to figure out the evolutionary pattern of a self-gravitating matter distribution. We must verify these forces whether they are in equilibrium or not [73, 74]. This phenomenon can be studied by constructing the Tolman-Oppenheimer-

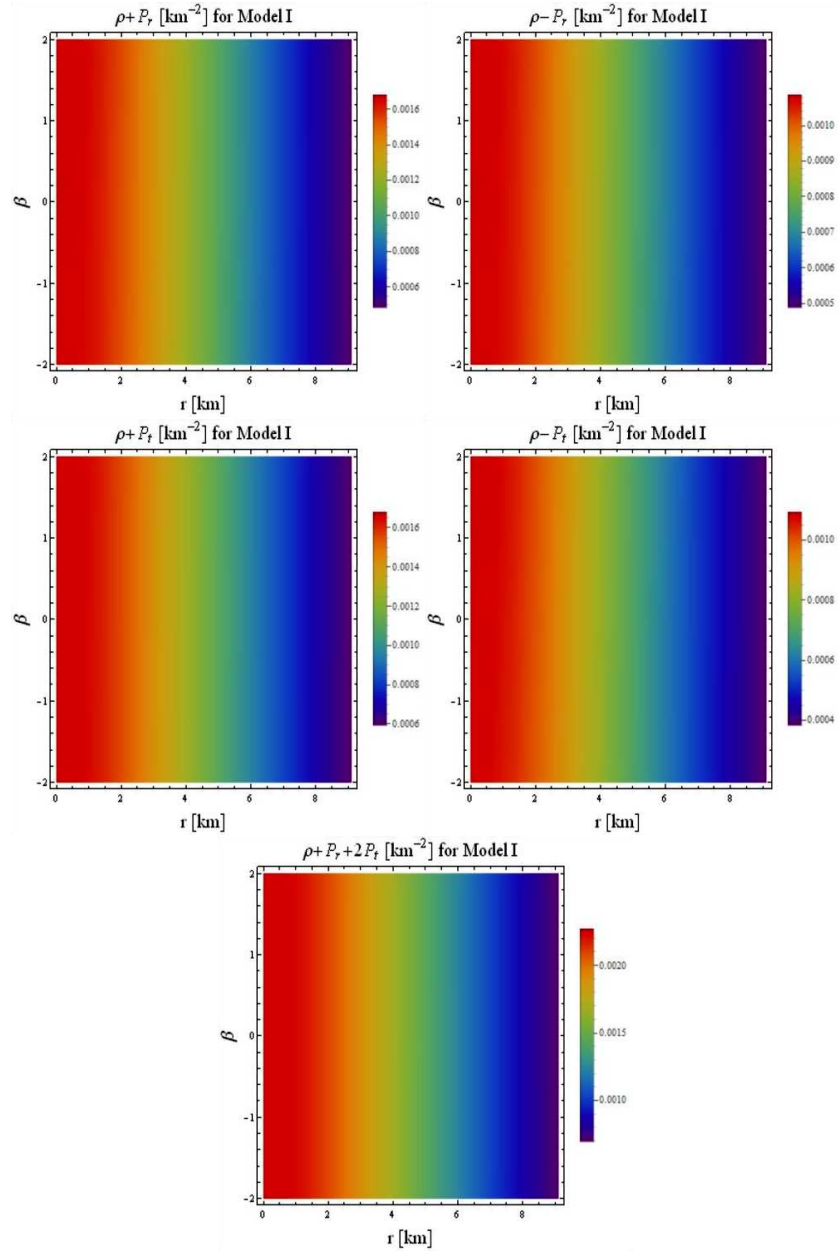


Figure 8: Energy conditions versus  $\beta$  and  $r$ .

Volkoff (TOV) equation. In the following, we calculate this through Eq.(4)

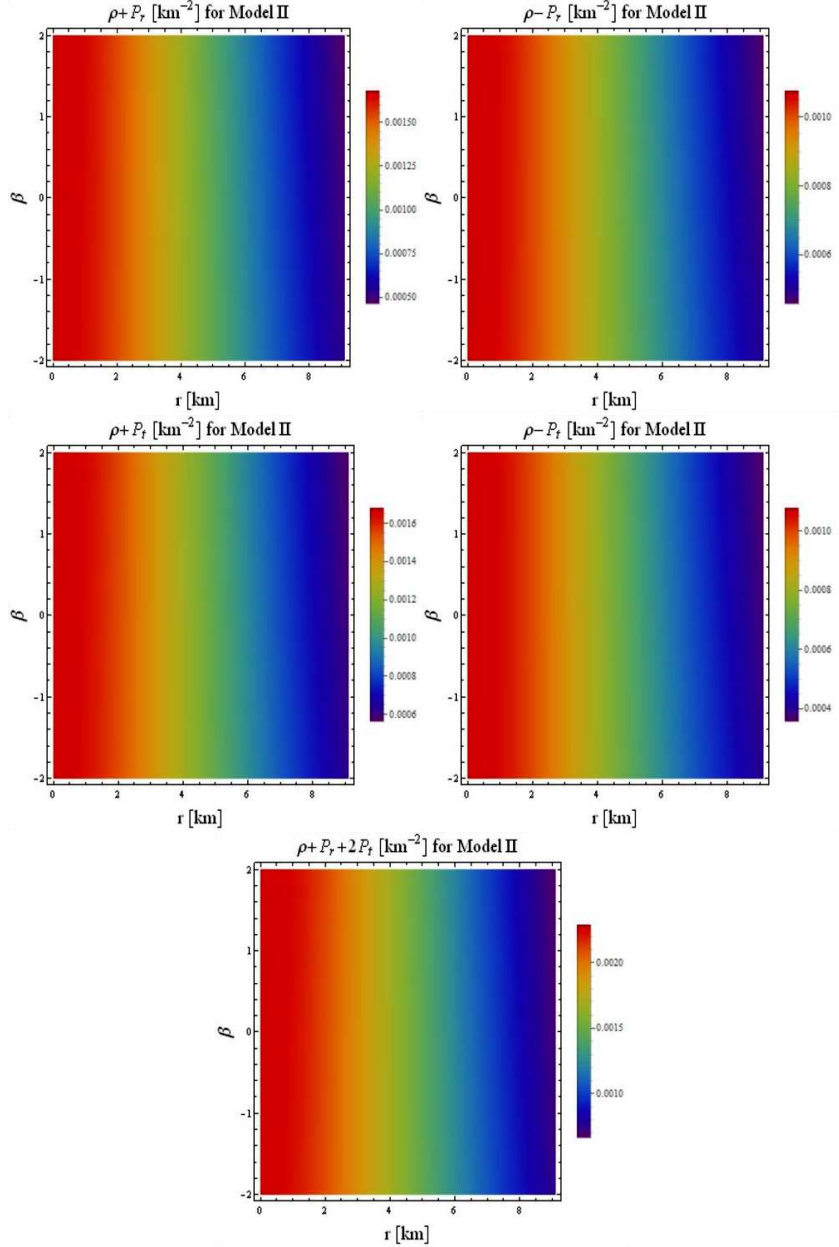


Figure 9: Energy conditions versus  $\beta$  and  $r$ .

with respect to both considered modified models, respectively, as

$$\frac{dP_r}{dr} + \frac{A'_1}{2}(\rho + P_r) - \frac{2}{r}(P_t - P_r) - \frac{2\beta e^{-A_2}}{\beta \mathcal{R} + 16\pi} \left[ \frac{A'_1 \rho}{8} \left( A_1'^2 - A'_1 A_2' + 2A_1'' + \frac{4A'_1}{r} \right) \right]$$

$$\begin{aligned}
& -\frac{\rho'}{8} \left( A_1'^2 - A_1' A_2' + 2A_1'' - \frac{4A_1'}{r} - \frac{8e^{A_2}}{r^2} + \frac{8}{r^2} \right) + P_r \left( \frac{5A_1'^2 A_2'}{8} - \frac{5A_1' A_2'^2}{8} + \frac{7A_1'' A_2'}{4} \right. \\
& - A_1' A_1'' + \frac{A_1' A_2''}{2} - \frac{5A_2'^2}{2r} - \frac{A_1'''}{2} + \frac{2A_2''}{r} + \frac{A_1' A_2'}{r} - \frac{A_2'}{r^2} - \frac{A_1''}{r} + \frac{A_1'}{r^2} + \frac{2e^{A_2}}{r^3} - \frac{2}{r^3} \Big) \\
& - \frac{P_r'}{8} \left( A_1'^2 - A_1' A_2' + 2A_1'' - \frac{4A_2'}{r} \right) + \frac{P_t}{r^2} \left( A_2' - A_1' + \frac{2e^{A_2}}{r} - \frac{2}{r} \right) - \frac{P_t'}{r} \left( \frac{A_2'}{2} - \frac{A_1'}{2} \right. \\
& \left. + \frac{e^{A_2}}{r} - \frac{1}{r} \right) = 0, \tag{31}
\end{aligned}$$

and

$$\begin{aligned}
& \frac{dP_r}{dr} + \frac{A_1'}{2} (\rho + P_r) - \frac{2}{r} (P_t - P_r) - \frac{2\beta}{\beta\mathcal{R}^2 + 16\pi} \left[ \rho \left\{ \frac{e^{-A_1-A_2} A_1' \mathcal{R} \mathcal{R}_{00}}{2} - e^{-2A_2} \right. \right. \\
& \times \mathcal{R}' \left( \frac{A_1'}{r} - \frac{e^{A_2}}{r^2} + \frac{1}{r^2} \right) \Big\} - \rho' \left\{ \frac{e^{-A_1-A_2} \mathcal{R} \mathcal{R}_{00}}{2} - e^{-2A_2} \mathcal{R} \left( \frac{A_1'}{r} - \frac{e^{A_2}}{r^2} + \frac{1}{r^2} \right) \right\} \\
& + P_r \left\{ \mathcal{R}' \mathcal{R}^{11} + \mathcal{R} (\mathcal{R}^{11})' - e^{-A_2} \mathcal{R} \mathcal{R}' + \frac{e^{-2A_2} A_2' \mathcal{R} \mathcal{R}_{11}}{2} \right\} - \frac{\mathcal{R} \mathcal{R}_{22}}{e^{A_2}} \left\{ \frac{P_t'}{r^2} - \frac{2P_t}{r^3} \right\} \\
& \left. + P_r' \left\{ \mathcal{R} \mathcal{R}^{11} - \frac{e^{-2A_2} \mathcal{R} \mathcal{R}_{11}}{2} \right\} \right] = 0. \tag{32}
\end{aligned}$$

The non-zero Ricci tensors  $\mathcal{R}_{00}$ ,  $\mathcal{R}_{11}$  and  $\mathcal{R}_{22}$  are provided in Appendix A. The compact form of the above TOV equations is

$$f_h + f_a + f_x = 0, \tag{33}$$

with  $f_h$  and  $f_a$  being hydrostatic and anisotropic forces, respectively, given by

$$f_h = -\frac{dP_r}{dr}, \quad f_a = \frac{2}{r} (P_t - P_r).$$

Moreover, we express the third force as  $f_x = f_g + f_e$ , where  $f_g$  and  $f_e$  are the gravitational and additional forces appearing due to modified theory, respectively. The force  $f_x$  contains all of the remaining terms of Eqs.(31) and (32) multiplied by a negative sign. Figure 10 guarantees that the developed solutions support the hydrostatic equilibrium in the interior of 4U 1820-30 compact star.

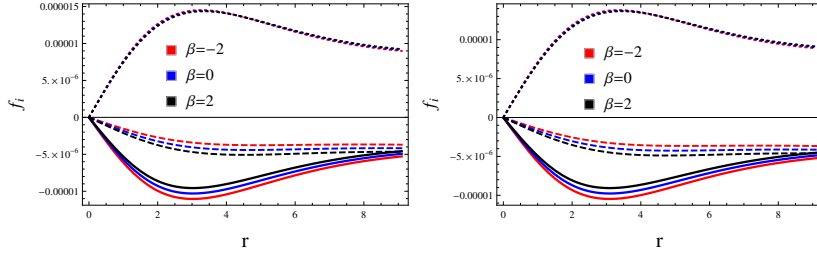


Figure 10: Variation in  $f_a$  (solid),  $f_h$  (dashed) and  $f_x$  (dotted) versus  $r$ .

## 4.7 Stability Analysis of 4U 1820-30 Compact Star

### 4.7.1 Causality and Cracking

In the vast realm of cosmic phenomena, particular attention has been devoted to celestial bodies and gravitational models that adhere to stability criteria. Numerous methodologies have been enlisted in the scientific literature to scrutinize the stability of these models. One essential condition that arises in these investigations is the causality criterion [75], which stipulates that the speed of light within any given medium must be less than the speed of light in a stable structure. This condition is often expressed mathematically as  $0 < v_s^2 < 1$ , and for anisotropic configurations, it takes the form of  $0 < v_{st}^2 < 1$  (tangential) and  $0 < v_{sr}^2 < 1$  (radial component). They are defined as

$$v_{st}^2 = \frac{dP_t}{d\rho}, \quad v_{sr}^2 = \frac{dP_r}{d\rho}. \quad (34)$$

Herrera [76] introduced the notion of cracking and put forth an inequality based on the previously defined parameters as  $0 < |v_{st}^2 - v_{sr}^2| < 1$ , which is applicable only to those objects that are in a stable state. In Figure 11, we observe graphical representations of the causality condition as well as cracking approach. The satisfaction of both these conditions ensures the stability of our resulting models for all  $\beta$  in the considered range.

### 4.7.2 Adiabatic Index

The adiabatic index, denoted by  $\Gamma$ , serves as a valuable tool for computing the stability of compact objects. This criterion has been widely utilized in the examination of self-gravitating structures, revealing a noteworthy findings. It has been determined that, in the context of stable objects, the lower limit

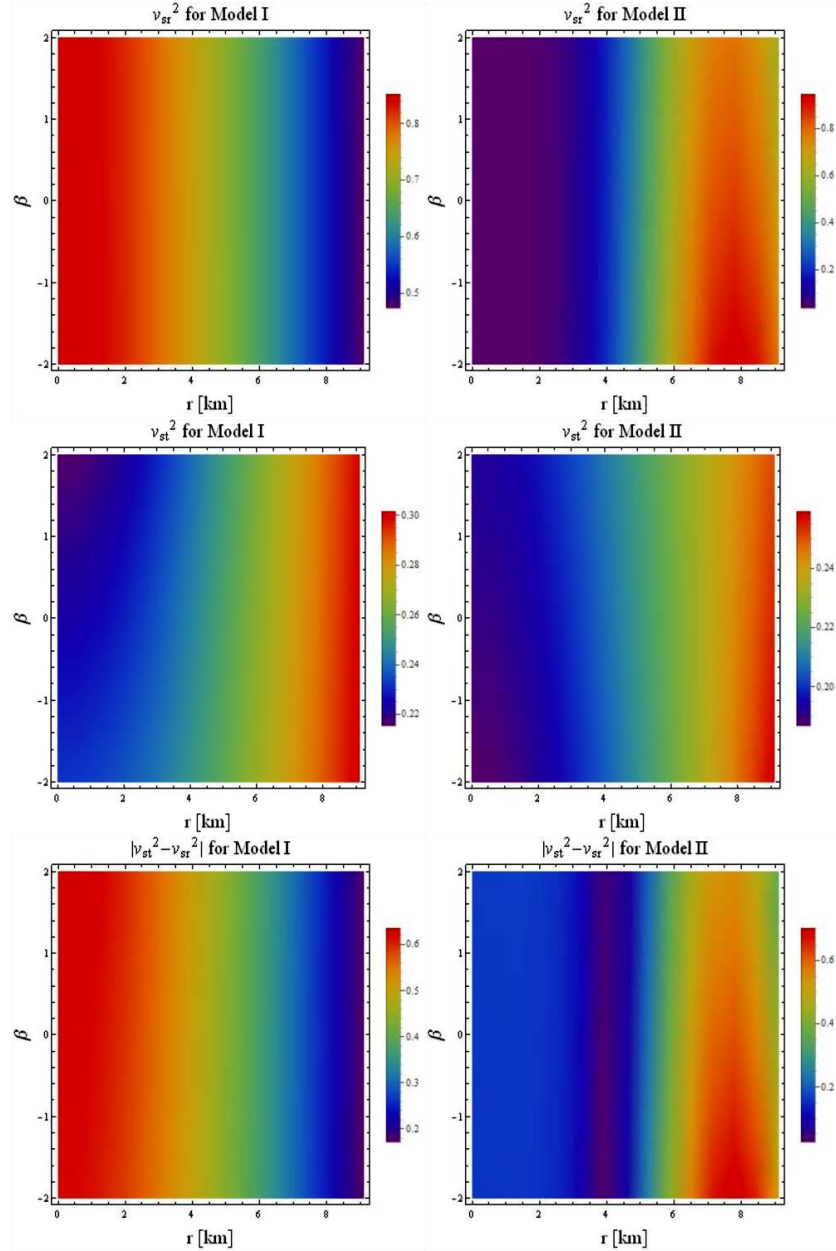


Figure 11: Stability analysis versus  $\beta$  and  $r$ .

of this index consistently remains at a value of  $\frac{4}{3}$  [77]. Here,  $\Gamma$  is divided into

two components for the case of anisotropic fluid. They are defined as

$$\Gamma_r = \frac{\rho + P_r}{P_r} \left( \frac{dP_r}{d\rho} \right), \quad \Gamma_t = \frac{\rho + P_t}{P_t} \left( \frac{dP_t}{d\rho} \right). \quad (35)$$

Figure 12 shows the stable behavior of both resulting models as they are consistent with the desired behavior of this index.

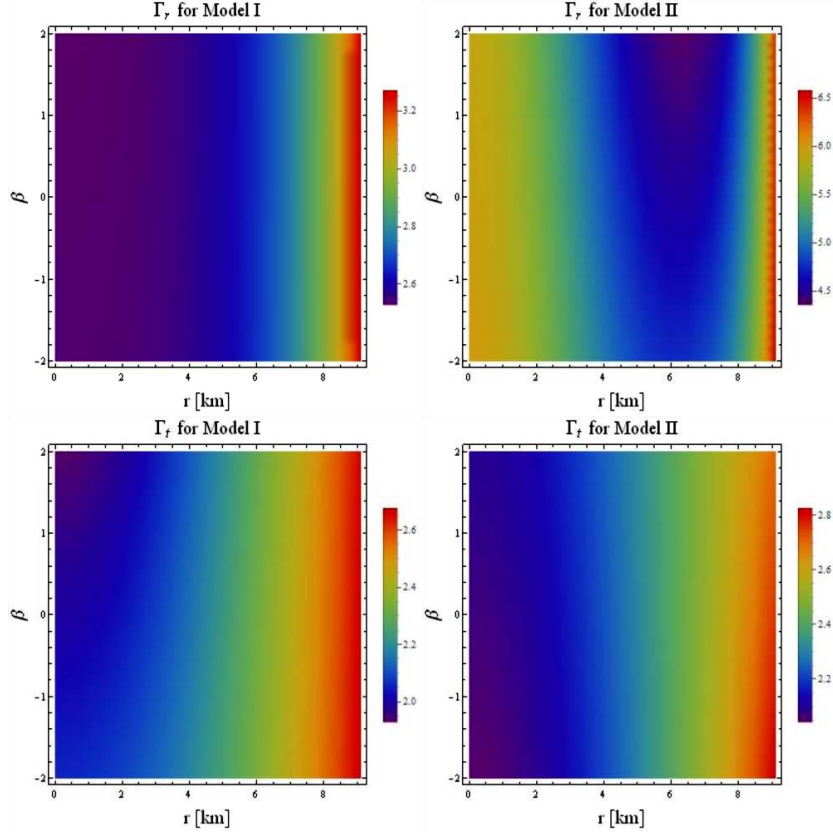


Figure 12: Adiabatic index versus  $\beta$  and  $r$ .

## 5 Estimating the Model Parameter

This section calculates the values of the model parameter for eight different compact stars which are consistent with their observed data such as radii and masses. We already discussed that there are two fundamental forms of

the matching conditions. The second form states that the radial pressure in any compact fluid configurations becomes zero at the boundary surface, i.e.,  $P_r \rightarrow 0$ . When we apply this condition on Eqs.(19), the resulting expression becomes

$$3M(R - 2M)^2 + 4B_c \{ 11\beta M^3 - M^2(8\pi R^3 + 11\beta R) + 3MR^2(\beta + 4\pi R^2) - 4\pi R^5 \} = 0, \quad (36)$$

and Eq.(21) takes the form after combining with the vanishing radial pressure constraint

$$B_c [2\beta M^5(4R^4 + 189R^2 - 198) + \beta M^4(487 - 20R^4 - 634R^2)R + 2M^3\{4\pi R^6 + \beta(8R^4 + 184R^2 - 91)R^2\} - M^2\{20\pi R^7 + \beta R^3(4R^4 + 85R^2 - 19)\}] + 2M(8\pi R^8 + 3\beta R^6) - 4[3MR^3(M - R)(R - 2M)^2] = 0. \quad (37)$$

We use Eqs.(36) and (37) to construct Tables **1** and **2**, providing the values of  $\beta$  for different compact stellar models corresponding to three different choices of the bag constant.

Table 1: Values of model parameter corresponding to different choices of the bag constant for model I.

Values of $B_c$		$75 \text{ MeV}/\text{fm}^3$	$85 \text{ MeV}/\text{fm}^3$	$95 \text{ MeV}/\text{fm}^3$
Star Models	Mass ( $M_\odot$ )	Radius (km)	$\beta$	$\beta$
Cen X-3	1.49	9.51	-151.814	149.225
SMC X-4	1.29	8.83	-401.983	-98.228
Her X-1	0.85	8.1	-826.024	-525.799
4U 1820-30	1.58	9.1	-459.042	-164.623
4U 1608-52	1.74	9.3	-427.304	-140.648
PSR J 1614 2230	1.97	10.3	5.949	289.672
PSR J 1903+327	1.67	9.82	-99.141	196.936
SAX J 1808.4-3658	0.9	7.95	-496.977	-189.679
				52.925

Table 2: Values of model parameter corresponding to different choices of the bag constant for model II.

Values of $B_c$		$75 \text{ MeV}/\text{fm}^3$	$85 \text{ MeV}/\text{fm}^3$	$95 \text{ MeV}/\text{fm}^3$
Star Models	Mass ( $M_\odot$ )	Radius (km)	$\beta$	$\beta$
Cen X-3	1.49	9.51	3.608	-3.547
SMC X-4	1.29	8.83	12.081	2.952
Her X-1	0.85	8.1	16.075	-0.846
4U 1820-30	1.58	9.1	10.449	3.747
4U 1608-52	1.74	9.3	8.543	2.812
PSR J 1614 2230	1.97	10.3	-0.095	-4.631
PSR J 1903+327	1.67	9.82	1.996	-3.965
SAX J 1808.4-3658	0.9	7.95	25.646	9.788
				-2.731

## 6 Conclusions

This study focuses on the possible existence of a specific compact object, 4U 1820-30, within the framework of  $f(\mathcal{R}, \mathcal{T}, \mathcal{R}_{\alpha\gamma}\mathcal{T}^{\alpha\gamma})$  theory. Two different modified models have been employed to explore the implications of the non-minimal interaction between matter and geometry, while considering a specific range of the coupling parameter  $\beta$ . We have derived the modified field equations (8)-(10) and (11)-(13) corresponding to both models and observed them as the under-determined systems. The Finch-Skea metric potentials, which satisfy the criteria [67], have been adopted to compute solutions for these sets. Additionally, we have utilized the MIT bag model to describe the internal distribution of strange stars. Within the Finch-Skea spacetime, characterized by three unknowns  $(d_1, d_2, d_3)$ , we have used the matching conditions at the hypersurface to calculate them in relation with the mass and radius of a self-gravitating star.

The graphical representation of the matter variables (Figure 2) ensures the validation of the obtained solutions (18)-(19) and (20)-(21). Examining the mass distribution within the strange star reveals a consistent outward increasing trend (Figure 6). We have also observed that model I exhibits a slightly denser interior in comparison to model II for the considered values of  $\beta$ . Furthermore, the plots of compactness and redshift fall within the acceptable limits. The EoS parameters (Figure 7) ensure the feasibility of the developed models. The energy bounds maintain positive values everywhere in the interior, confirming the physical viability of both of our proposed solutions (Figures 8 and 9). Moreover, the TOV equations (31) and (32) have been plotted (Figure 10) and it has been shown that the obtained

models agree with the hydrostatic equilibrium condition in the presence of modified corrections.

Finally, we have employed three distinct criteria to assess the stability within this framework. Their plots demonstrated the stability of the solutions (18)-(19) and (20)-(21), as supported by the observations (Figures 11 and 12), in agreement with [34, 53]. Notably, it becomes apparent that our solutions exhibit superior efficacy in comparison to those proposed in [27], suggesting that the additional force within this theoretical framework may yield more favorable results for the considered parametric values. Further, it is important to note here that there are several past related works on compact stars. In the following, we highlight two main differences which set our work different from them. Firstly, we have used the disappearing radial pressure condition at the spherical boundary to estimate the values of the model parameter that correspond to the observed data (masses and radii) of eight different compact stars. Tables 1 and 2 present these parametric values for models I and II, respectively, for different acceptable values of the bag constant. It is found that  $\beta$  takes both negative and positive values, indicating itself to be an arbitrary parameter. Secondly, in the recent works, the compact interiors have not been explored for our model II. We have adopted this model for the very first time in this article and presented a brief comparison with the results corresponding to the first model. Our findings can ultimately be reduced to GR when  $\beta = 0$ .

## Appendix A

The values of  $\tau_i'^s$  displayed in Eqs.(11)-(13) are

$$\begin{aligned}\tau_1 &= \frac{e^{-A_2}}{4} \left( A_1'^2 - A_1' A_2' + 2A_1'' + \frac{4A_1'}{r} \right), \\ \tau_2 &= \frac{e^{-A_2}}{4} \left( A_1' A_2' - A_1'^2 - 2A_1'' + \frac{4A_2'}{r} \right), \\ \tau_3 &= e^{-A_2} \left( \frac{A_2'}{r} - \frac{A_1'}{r} + \frac{2e^{A_2}}{r^2} - \frac{2}{r^2} \right), \\ \tau_4 &= \frac{e^{-A_2}}{4} \left( A_1' A_2'^2 - A_1'^2 A_2' - 3A_1'' A_2' - A_1' A_2'' + 2A_1' A_1'' + 2A_1''' - \frac{4A_1'}{r^2} \right. \\ &\quad \left. - \frac{4A_1' A_2'}{r} + \frac{4A_1''}{r} \right),\end{aligned}$$

$$\begin{aligned}
\tau_5 &= \frac{e^{-A_2}}{4} \left( A_1'^2 A_2' - A_1' A_2'^2 + 3A_1'' A_2' + A_1' A_2'' - 2A_1' A_1'' - 2A_1''' - \frac{4A_2'}{r^2} \right. \\
&\quad \left. - \frac{4A_2'^2}{r} + \frac{4A_2''}{r} \right), \\
\tau_6 &= e^{-A_2} \left( \frac{A_1' A_2'}{r} - \frac{4A_2' e^{A_2}}{r^2} - \frac{A_2'^2}{r} + \frac{A_2''}{r} + \frac{A_2'}{r^2} - \frac{A_1''}{r} + \frac{A_1'}{r^2} - \frac{4e^{A_2}}{r^3} + \frac{4}{r^3} \right), \\
\tau_7 &= \frac{e^{-A_2}}{4} \left( A_1'^2 A_2'^2 - A_1' A_2'^3 + 4A_1'' A_2'^2 + 3A_1' A_2' A_2'' - 5A_1''' A_2' - 4A_1'' A_2'' \right. \\
&\quad \left. - A_1'^2 A_2'' - A_1' A_2''' - 4A_1' A_1'' A_2' + 2A_1''^2 + 2A_1' A_1''' + 2A_1'''' + \frac{4A_1' A_2'^2}{r} \right. \\
&\quad \left. - \frac{8A_1'' A_2'}{r} - \frac{4A_1' A_2''}{r} + \frac{4A_1'''}{r} - \frac{8A_1''}{r^2} + \frac{8A_1'}{r^3} \right), \\
\tau_8 &= \frac{e^{-A_2}}{4} \left( A_1' A_2'^3 - A_1'^2 A_2'^2 - 4A_1'' A_2'^2 - 3A_1' A_2' A_2'' + 4A_1' A_1'' A_2' + 5A_1''' A_2' \right. \\
&\quad \left. + A_1'^2 A_2'' + A_1' A_2''' + 4A_1'' A_2'' - 2A_1''^2 - 2A_1' A_1''' - 2A_1'''' + \frac{4A_2'^3}{r} - \frac{12A_2' A_2''}{r} \right. \\
&\quad \left. + \frac{8A_2'^2}{r^2} + \frac{4A_2'''}{r} - \frac{8A_2''}{r^2} + \frac{8A_2'}{r^3} \right), \\
\tau_9 &= e^{-A_2} \left( \frac{A_2'^3}{r} - \frac{A_1' A_2'^2}{r} - \frac{3A_2' A_2''}{r} + \frac{4A_1'' A_2'}{r} - \frac{2A_1' A_2'}{r^2} - \frac{6A_2'}{r^3} + \frac{A_1' A_2''}{r} \right. \\
&\quad \left. - \frac{A_2'' e^{A_2}}{r^2} + \frac{8A_2' e^{A_2}}{r^3} + \frac{A_2'''}{r} - \frac{A_1'''}{r} + \frac{2A_1''}{r^2} - \frac{2A_1'}{r^3} + \frac{12e^{A_2}}{r^4} - \frac{12}{r^4} \right).
\end{aligned}$$

The Ricci scalar and non-zero components of Ricci tensor for metric (6) are

$$\begin{aligned}
\mathcal{R} &= \frac{1}{2e^{A_2}} \left( A_1'^2 - A_2' A_1' + 2A_1'' - \frac{4A_2'}{r} + \frac{4A_1'}{r} - \frac{4e^{A_2}}{r^2} + \frac{4}{r^2} \right), \\
\mathcal{R}_{00} &= \frac{1}{4e^{A_2-A_1}} \left( A_1'^2 - A_2' A_1' + 2A_1'' + \frac{4A_1'}{r} \right), \\
\mathcal{R}_{11} &= \frac{1}{4} \left( A_2' A_1' - A_1'^2 - 2A_1'' + \frac{4A_2'}{r} \right), \quad \mathcal{R}_{22} = \frac{1}{2e^{A_2}} \left( A_2' r - A_1' r + 2e^{A_2} - 2 \right).
\end{aligned}$$

## Appendix B

The anisotropy corresponding to the model I is expressed by

$$\begin{aligned} \Pi = & \left\{ (2\beta r A_1'' - \beta A_2' (r A_1' + 4) + \beta r A_1'^2 + 4\beta A_1' + 32\pi r e^{A_2}) (2(8\beta - \beta r^2 A_2'' \right. \\ & + 9\beta r^2 A_1'' + 64\pi r^2 e^{A_2} - 8\beta e^{A_2}) - \beta r^2 A_2'^2 + r^2 3\beta A_1'^2 - 10\beta r A_2' (r A_1' + 4) \\ & \left. + 16\beta r A_1') \right\}^{-1} \left\{ 3\beta r^3 (6\beta B_c + 1) A_1'^4 + 4r (\beta A_2'' (8B_c (\beta + (8\pi r^2 - \beta) e^{A_2}) + r^2 \right. \\ & \times (4\beta B_c - 1) A_1'') + 8A_1'' (\beta (1 + \beta B_c) + e^{A_2} (8\pi r^2 (3\beta B_c + 1) - \beta (\beta B_c + 1))) \\ & + 128\pi B_c e^{A_2} ((8\pi r^2 - \beta) e^{A_2} + \beta) + \beta r^2 (10\beta B_c + 9) A_1'^2) + 2r A_1'^2 (4(2(2\beta \\ & \times (3\beta B_c + 1) + (2B_c \beta + 1) (8\pi r^2 - \beta) e^{A_2}) + \beta r^2 (7\beta B_c + 3) A_1'') - \beta r^2 A_2'' \\ & \times (6\beta B_c + 1)) + 4A_1' (8(\beta (2\beta B_c + 1) + e^{A_2} (4\pi r^2 (8\beta B_c + 1) - \beta (2\beta B_c + 1))) \\ & + r^2 (24\beta B_c + 19) \beta A_1'' - 3\beta r^2 A_2'') + \beta r^2 A_2'^3 (88\beta B_c + (22\beta B_c r + r) A_1' + 14) \\ & + \beta r A_2'^2 (-2(8(B_c (\beta + 24\pi r^2) e^{A_2} - 9\beta B_c - 4) + (22\beta B_c + 1) A_1'' (r) r^2) + 9r^2 \\ & \times A_1'^2 (2\beta B_c + 1) + 6r (8\beta B_c + 11) A_1') + 2\beta r^2 (16\beta B_c + 19) A_1'^3 - A_2' (\beta r^3 A_1'^3 \\ & \times (34\beta B_c + 13) + 4(\beta r^2 (12\beta B_c + 1) A_2'' + 8(\beta (2\beta B_c + 1) - e^{A_2} (\beta (1 + 2\beta B_c) \\ & - 12\pi r^2 (4\beta B_c + 1)))) + \beta r^2 (44\beta B_c + 27) A_1'') + 2r A_1' (\beta r^2 (6\beta B_c - 1) A_2'' + 8 \\ & \times (\beta (13\beta B_c + 10) + e^{A_2} (8\pi r^2 (3\beta B_c + 1) - \beta (\beta B_c + 1))) + \beta (22\beta B_c + 19) \\ & \times r^2 A_1'') + 2\beta r^2 (92\beta B_c + 35) A_1'^2) \right\}, \end{aligned}$$

whereas it becomes for model II as

$$\begin{aligned} \Pi = & \left\{ 2e^{A_2} r^2 \beta \mathcal{R}^2 + 4\beta (r A_2' + 2e^{A_2} - r A_1' - 2) \mathcal{R} + r (\beta (r \mathcal{R}' - 2r \tau_6 - 4\tau_3) A_1' \right. \\ & - r \beta \tau_3 A_1'^2 + 32e^{A_2} \pi r - 4r \beta \tau_9 - 4\beta \tau_6 + \beta A_2' (r A_1' \tau_3 + 4\tau_3 + 2r \tau_6 - r \mathcal{R}') + 2r \\ & \times \beta \mathcal{R}'' - 2r \beta \tau_3 A_1'' \right\}^{-1} \left\{ r (r A_1'^2 + 2A_1' - A_2' (r A_1' + 2) + 2r A_1'') \right\} + \left\{ 8e^{A_2} r \beta \mathcal{R}^2 \right. \\ & + \beta (A_2' (7r A_1' - 4) - r A_1'^2 - 20A_1' - 8r A_1'') \mathcal{R} + 2(2\beta \tau_8 r - 3\beta \tau_4 A_1' r - \beta \tau_5 A_1' r \\ & + 2\beta \mathcal{R}'' r + 64e^{A_2} \pi r - \beta (6\tau_1 + 2\tau_2 + 3r \tau_4 + r \tau_5) A_2' - \beta \mathcal{R}' (r A_2' + r A_1' - 4) \\ & - 6\beta \tau_1 A_1' - 2\beta \tau_2 A_1') \right\}^{-1} \left\{ 4(2e^{A_2} r \beta B_c \mathcal{R}^2 + \beta B_c (2A_2' (r A_1' - 2) - r A_1'^2 - 8A_1' \right. \\ & \left. - 2r A_1'') \mathcal{R} + 32e^{A_2} \pi r B_c + 4r \beta B_c \tau_7 - 4\beta B_c \tau_1 A_2' - 2r \beta B_c \tau_4 A_2' - A_2' - 4\beta B_c \tau_1 \right. \end{aligned}$$

$$\begin{aligned}
& \times A'_1 - 2r\beta B_c \tau_4 A'_1 - A'_1 - \beta B_c R' (r A_2' + r A'_1 - 4) + 2r\beta B_c \mathcal{R}'' \Big\} + \Big\{ (8e^{A_2} r \beta \mathcal{R}^2 \\
& + \beta (-r A_1'^2 - 20A'_1 + A_2' (7r A'_1 - 4) - 8r A''_1) \mathcal{R} + 2(2\beta \tau_8 r - 3\beta \tau_4 A'_1 r - \beta \tau_5 A'_1 r \\
& + 2\beta \mathcal{R}'' r + 64e^{A_2} \pi r - \beta(6\tau_1 + 2\tau_2 + 3r\tau_4 + r\tau_5) A_2' - 6\beta \tau_1 A'_1 - 2\beta \tau_2 A'_1 - \beta \mathcal{R}' \\
& \times (r A_2' + r A'_1 - 4)) (2e^{A_2} r^2 \beta \mathcal{R}^2 + 4\beta (r A_2' + 2e^{A_2} - r A'_1 - 2) \mathcal{R} - r(r \beta \tau_3 A_1'^2 \\
& - \beta (-4\tau_3 - 2r\tau_6 + r\mathcal{R}')) A'_1 - 32e^{A_2} \pi r + 4r\beta \tau_9 + 4\beta \tau_6 - \beta A_2' (r A'_1 \tau_3 + 2r\tau_6 \\
& + 4\tau_3 - r\mathcal{R}') - 2r\beta \mathcal{R}'' + 2r\beta \tau_3 A''_1)) \Big\}^{-1} \Big\{ 2r\beta ((-r(2\tau_1 + \mathcal{R}) A_1'^2 - (4\tau_1 + r4\tau_4 \\
& - 2r\mathcal{R}') A'_1 - 8r\tau_7 - 8\tau_4 + A_2' (2r A'_1 \tau_1 + 4\tau_1 + 4r\tau_4 + \mathcal{R}(r A'_1 + 4)) - r4\tau_1 A'_1 \\
& - 2r\mathcal{R} A''_1) (2e^{A_2} r \beta B_c \mathcal{R}^2 + \beta B_c (2r A_1'^2 + 4A'_1 + A_2' (r A'_1 + 8) - 2r A''_1) \mathcal{R} - 3A'_2 \\
& - 32e^{A_2} \pi r B_c + 4r\beta B_c \tau_8 - 4\beta B_c \tau_2 A_2' - 2r\beta B_c \tau_5 A_2' - 4\beta B_c \tau_2 A'_1 - 2r\beta \tau_5 B_c A'_1 \\
& - 3A'_1 + \beta B_c \mathcal{R}' (r A_2' + r A'_1 - 4) - 2r\beta B_c \mathcal{R}'')) + (2r\tau_2 A_1'^2 - r\mathcal{R} A_1'^2 + 4\tau_2 A'_1 + 8\tau_5 \\
& + 4r\tau_5 A'_1 - 4\mathcal{R} A'_1 + 8r\tau_8 + 2\mathcal{R}' (r A_2' - 2r A'_1 - 4) + ((\mathcal{R} - 2\tau_2) r A'_1 - 4(\tau_2 + r\tau_5)) \\
& \times A_2' - 4r\mathcal{R}'' + 4r\tau_2 A''_1 - 2r\mathcal{R} A''_1) (-2e^{A_2} r \beta B_c \mathcal{R}^2 + \beta B_c (A_1'^2 r + 8A'_1 + 2r A''_1 \\
& + A_2' (4 - 2r A'_1)) \mathcal{R} - 32e^{A_2} \pi r B_c - 4r\beta B_c \tau_7 + 4\beta B_c \tau_1 A_2' + 2r\beta B_c \tau_4 A_2' + A_2' \\
& + 4\beta B_c \tau_1 A'_1 + 2r\beta B_c \tau_4 A'_1 + A'_1 + \beta B_c \mathcal{R}' (r A_2' + r A'_1 - 4) - 2r\beta B_c \mathcal{R}'') \Big\}.
\end{aligned}$$

**Data Availability Statement:** This manuscript has no associated data.

## References

- [1] H.A. Buchdahl, Non-linear Lagrangians and cosmological theory, *Mon. Not. R. Astron. Soc.* 150 (1970) 1-8.
- [2] S. Nojiri, S.D. Odintsov, Modified gravity with negative and positive powers of curvature: Unification of inflation and cosmic acceleration, *Phys. Rev. D* 68 (2003) 123512.
- [3] Y.S. Song, W. Hu, I. Sawicki, Large scale structure of  $f(R)$  gravity, *Phys. Rev. D* 75 (2007) 044004.
- [4] M. Sharif, H.R. Kausar, Effects of  $f(R)$  model on the dynamical instability of expansionfree gravitational collapse, *J. Cosmol. Astropart. Phys.* 07 (2011) 022.

- [5] A.V. Astashenok, S. Capozziello, S.D. Odintsov, Maximal neutron star mass and the resolution of the hyperon puzzle in modified gravity, *Phys. Rev. D* 89 (2014) 103509.
- [6] S. Capozziello, S. Nojiri, S.D. Odintsov, A. Troisi, Cosmological viability of  $f(R)$ -gravity as an ideal fluid and its compatibility with a matter dominated phase, *Phys. Lett. B* 639 (2006) 135.
- [7] J.D. Barrow, S. Hervik, Anisotropically inflating universes, *Phys. Rev. D* 73 (2006) 023007.
- [8] M. Visser, Energy conditions in the epoch of galaxy formation, *Science* 276 (1997) 88.
- [9] J. Santos, J.S. Alcaniz, M.J. Reboucas, Energy conditions and supernovae observations, *Phys. Rev. D* 74 (2006) 067301.
- [10] O. Bertolami, C.G. Boehmer, T. Harko, F.S.N. Lobo, Extra force in  $f(R)$  modified theories of gravity, *Phys. Rev. D* 75 (2007) 104016.
- [11] T. Harko, F.S.N. Lobo, S. Nojiri, S.D. Odintsov,  $f(R, T)$  gravity, *Phys. Rev. D* 84 (2011) 024020.
- [12] M. Sharif, M. Zubair, Thermodynamic behavior of particular  $f(R, T)$ -gravity models, *J. Exp. Theor. Phys.* 117 (2013) 248-257.
- [13] H. Shabani, M. Farhoudi,  $f(R, T)$  cosmological models in phase space, *Phys. Rev. D* 88 (2013) 044048.
- [14] A. Das, S. Ghosh, B.K. Guha, S. Das, F. Rahaman, S. Ray, Gravastars in  $f(R, T)$  gravity, *Phys. Rev. D* 95 (2017) 124011.
- [15] S.K. Maurya, A. Banerjee, F. Tello-Ortiz, Buchdahl model in  $f(R, T)$  gravity: A comparative study with standard Einstein gravity, *Phys. Dark Universe* 27 (2020) 100438.
- [16] P. Rej, P. Bhar, Charged strange star in  $f(R, T)$  gravity with linear equation of state, *Astrophys. Space Sci.* 366 (2021) 35.
- [17] M. Sharif, T. Naseer, Isotropization and complexity analysis of decoupled solutions in  $f(R, T)$  theory, *Eur. Phys. J. Plus* 137 (2022) 1304.

- [18] M. Sharif, T. Naseer, Anisotropic complexity-free models in modified  $f(R, T)$  theory, *Ann. Phys.* 459 (2023) 169527.
- [19] M. Sharif, T. Naseer, Impact of charge on complexity analysis and isotropic decoupled solutions in gravity, *Phys. Scr.* 98 (2023) 115012.
- [20] M. Sharif, T. Naseer, Effect of extended gravitational decoupling on isotropization and complexity in  $f(R, T)$  theory, *Class. Quantum Grav.* 40 (2023) 035009.
- [21] T. Naseer, M. Sharif, Study of Decoupled Cosmological Solutions in  $f(R, T)$  Theory, *Fortschr. Phys.* 71 (2023) 2300004.
- [22] Z. Haghani, T. Harko, F.S.N. Lobo, H.R. Sepangi, S. Shahidi, Further matters in space-time geometry:  $f(R, T, R_{\mu\nu}T^{\mu\nu})$  gravity, *Phys. Rev. D* 88 (2013) 044023.
- [23] M. Sharif, M. Zubair, Study of thermodynamic laws in  $f(R, T, R_{\mu\nu}T^{\mu\nu})$  gravity, *J. Cosmol. Astropart. Phys.* 11 (2013) 042.
- [24] S.D. Odintsov, D. Saez-Gomez,  $f(R, T, R_{\mu\nu}T^{\mu\nu})$  gravity phenomenology and  $\Lambda$ CDM universe, *Phys. Lett. B* 725 (2013) 437-444.
- [25] I. Ayuso, J.B. Jimenez, A. De la Cruz-Dombriz, Consistency of universally nonminimally coupled  $f(R, T, R_{\mu\nu}T^{\mu\nu})$  theories, *Phys. Rev. D* 91 (2015) 104003.
- [26] E.H. Baffou, M.J.S. Houndjo, J. Tossa, Exploring stable models in  $f(R, T, R_{\mu\nu}T^{\mu\nu})$  gravity, *Astrophys. Space Sci.* 361 (2016) 376.
- [27] M. Sharif, A. Waseem, Physical behavior of anisotropic compact stars in  $f(R, T, R_{\mu\nu}T^{\mu\nu})$  gravity, *Can. J. Phys.* 94 (2016) 1024-1039.
- [28] Z. Yousaf, M.Z. Bhatti, T. Naseer, Study of static charged spherical structure in  $f(R, T, Q)$  gravity, *Eur. Phys. J. Plus* 135 (2020) 353.
- [29] Z. Yousaf, M.Z. Bhatti, T. Naseer, Evolution of the charged dynamical radiating spherical structures, *Ann. Phys.* 420 (2020) 168267.
- [30] Z. Yousaf, M.Y. Khlopov, M.Z. Bhatti, T. Naseer, Influence of modification of gravity on the complexity factor of static spherical structures, *Mon. Not. R. Astron. Soc.* 495 (2020) 4334-4346.

- [31] Z. Yousaf, M.Z. Bhatti, T. Naseer, New definition of complexity factor in  $f(R, T, R_{\mu\nu}T^{\mu\nu})$  gravity, *Phys. Dark Universe* 28 (2020) 100535.
- [32] Z. Yousaf, M.Z. Bhatti, T. Naseer, I. Ahmad, The measure of complexity in charged celestial bodies in  $f(R, T, R_{\mu\nu}T^{\mu\nu})$  gravity, *Phys. Dark Universe* 29 (2020) 100581.
- [33] Z. Yousaf, M.Z. Bhatti, T. Naseer, Measure of complexity for dynamical self-gravitating structures, *Int. J. Mod. Phys. D* 29 (2020) 2050061.
- [34] M. Sharif, T. Naseer, Effects of non-minimal matter-geometry coupling on embedding class-one anisotropic solutions, *Phys. Scr.* 97 (2022) 055004.
- [35] M. Sharif, T. Naseer, Influence of charge on anisotropic class-one solution in non-minimally coupled gravity, *Phys. Scr.* 97 (2022) 125016.
- [36] M. Sharif, T. Naseer, Extended decoupled anisotropic solutions in  $f(R, T, R_{\gamma\chi}T^{\gamma\chi})$  gravity, *Int. J. Mod. Phys. D* 31 (2022) 2240017.
- [37] M. Sharif, T. Naseer, Study of charged compact stars in non-minimally coupled gravity, *Fortschr. Phys.* 71 (2023) 2200147.
- [38] W. Baade, F. Zwicky, Remarks on super-novae and cosmic rays, *Phys. Rev.* 46 (1934) 76.
- [39] E. Witten, Cosmic separation of phases, *Phys. Rev. D* 30 (1984) 272.
- [40] A.R. Bodmer, Collapsed nuclei, *Phys. Rev. D* 4 (1971) 1601.
- [41] C. Alcock, E. Farhi, A. Olinto, Strange stars, *Astrophys. J.* 310 (1986) 261.
- [42] I. Bombaci, Observational evidence for strange matter in compact objects from the x-ray burster 4U 1820-30, *Phys. Rev. C* 55 (1997) 1587.
- [43] M. Dey, I. Bombaci, J. Dey, S. Ray, B.C. Samanta, Strange stars with realistic quark vector interaction and phenomenological density-dependent scalar potential, *Phys. Lett. B* 438 (1998) 123.
- [44] B. Das, P.C. Ray, I. Radinschi, F. Rahaman, S. Ray, Isotropic cases of static charged fluid spheres in general relativity, *Int. J. Mod. Phys. D* 20 (2011) 1675.

- [45] G.H. Bordbar, A.R. Peivand, Computation of the structure of a magnetized strange quark star, *Res. Astron. Astrophys.* 11 (2011) 851.
- [46] P. Haensel, J.L. Zdunik, R. Schaefer, Strange quark stars, *Astron. Astrophys.* 160 (1986) 121.
- [47] K.S. Cheng, Z.G. Dai, T. Lu, Strange stars and related astrophysical phenomena, *Int. J. Mod. Phys. D* 7 (1998) 139.
- [48] M.K. Mak, T. Harko, An exact anisotropic quark star model, *Chin. J. Astron. Astrophys.* 2 (2002) 248.
- [49] P. Rej, P. Bhar, Model of hybrid star with baryonic and strange quark matter in Tolman-Kuchowicz spacetime, *Int. J. Geom. Methods Mod.* 19 (2022) 2250104.
- [50] P. Rej, A. Errehymy, M. Daoud, Charged strange star model in Tolman-Kuchowicz spacetime in the background of 5D Einstein-Maxwell-Gauss-Bonnet gravity, *Eur. Phys. J. C* 83 (2023) 392.
- [51] P.B. Demorest, T. Pennucci, S.M. Ransom, M.S.E. Roberts, J.W.T. Hessels, A two-solar-mass neutron star measured using Shapiro delay, *Nature* 467 (2010) 1081.
- [52] F. Rahaman, K. Chakraborty, P.K.F. Kuhfittig, G.C. Shit, M. Rahman, A new deterministic model of strange stars, *Eur. Phys. J. C* 74 (2014) 3126.
- [53] M. Sharif, A. Waseem, Anisotropic quark stars in  $f(R, T)$  gravity, *Eur. Phys. J. C* 78 (2018) 868.
- [54] M. Sharif, A. Majid, Anisotropic strange stars through embedding technique in massive Brans-Dicke gravity, *Eur. Phys. J. Plus* 135 (2020) 558.
- [55] M.R. Finch, J.E.F. Skea, A realistic stellar model based on an ansatz of Duorah and Ray, *Class. Quantum Grav.* 6 (1989) 467.
- [56] A. Banerjee, F. Rahaman, K. Jotania, R. Sharma, I. Karar, Finch-Skea star in dimensions, *Gen. Relativ. Gravit.* 45 (2013) 717.

- [57] S. Hansraj, S.D. Maharaj, Charged analogue of Finch-Skea stars, *Int. J. Mod. Phys. D* 15 (2006) 1311.
- [58] P. Bhar, K.N. Singh, F. Rahaman, N. Pant, S. Banerjee, A charged anisotropic well-behaved Adler-Finch-Skea solution satisfying Karmarkar condition, *Int. J. Mod. Phys. D* 26 (2017) 1750078.
- [59] M.F. Shamir, G. Mustafa, M Ahmad, Charged anisotropic Finch-Skea-Bardeen spheres, *Nucl. Phys. B* 967 (2021) 115418.
- [60] S. Dey, A. Chanda, B.C. Paul, Compact objects in  $f(R, T)$  gravity with Finch-Skea geometry, *Eur. Phys. J. Plus* 136 (2021) 228.
- [61] M. Sharif, S. Manzoor, Compact objects admitting Finch-Skea symmetry in  $f(R, T^2)$  gravity, *Ann. Phys.* 454 (2023) 169337.
- [62] C.W. Misner, D.H. Sharp, Relativistic equations for adiabatic, spherically symmetric gravitational collapse, *Phys. Rev.* 136 (1964) B571.
- [63] N.K. Glendenning, First-order phase transitions with more than one conserved charge: Consequences for neutron stars, *Phys. Rev. D* 46 (1992) 1274.
- [64] J.M. Lattimer, M. Prakash, Neutron star structure and the equation of state, *Astrophys. J.* 550 (2001) 426.
- [65] M. Kalam, A.A. Usmani, F. Rahaman, S.M. Hossein, I. Karar, R. Sharma, A relativistic model for strange quark star, *Int. J. Theor. Phys.* 52 (2013) 3319.
- [66] J.D.V. Arbanil, M. Malheiro, Radial stability of anisotropic strange quark stars, *J. Cosmol. Astropart. Phys.* 11 (2016) 012.
- [67] K. Lake, All static spherically symmetric perfect-fluid solutions of Einstein equations, *Phys. Rev. D* 67 (2003) 104015.
- [68] T. Guver, P. Wroblewski, L. Camarota, F. Ozel, The Mass and Radius of the Neutron Star in 4U 1820-30, *Astrophys. J.* 719 (2010) 1807.
- [69] M. Sharif, T. Naseer, Effects of  $f(R, T, R_{\gamma\nu}T^{\gamma\nu})$  gravity on anisotropic charged compact structures, *Chin. J. Phys.* 73 (2021) 179.

- [70] T. Naseer, M. Sharif, Study of Decoupled Anisotropic Solutions in  $f(R, T, R_{\rho\eta}T^{\rho\eta})$  Theory, *Universe* 8 (2022) 62.
- [71] H.A. Buchdahl, General relativistic fluid spheres, *Phys. Rev.* 116 (1959) 1027.
- [72] B.V. Ivanov, Maximum bounds on the surface redshift of anisotropic stars, *Phys. Rev. D* 65 (2002) 104011.
- [73] F. Tello-Ortiz, S.K. Maurya, Y. Gomez-Leyton, Class I approach as MGD generator, *Eur. Phys. J. C* 80 (2020) 324.
- [74] B. Dayanandan, T.T. Smitha, S.K. Maurya, Self-gravitating anisotropic star using gravitational decoupling, *Phys. Scr.* 96 (2021) 125041.
- [75] H. Abreu, H. Hernandez, L.A. Nunez, Sound speeds, cracking and the stability of self-gravitating anisotropic compact objects, *Class. Quantum Grav.* 24 (2007) 4631
- [76] L. Herrera, Cracking of self-gravitating compact objects, *Phys. Lett. A* 165 (1992) 206.
- [77] H. Heintzmann, W. Hillebrandt, Neutron stars with an anisotropic equation of state-Mass, redshift and stability, *Astron. Astrophys.* 38 (1975) 51-55.